University of California

Santa Barbara

Exploring structural modifications and biomarkers to optimize and expand the E-DNA scaffold sensor for applications in point of care serology

A thesis submitted in partial satisfaction of the requirements for the degree

Master of Science in Chemistry

By

Ava Shruti Kartik Greenwood

Committee in charge:

Professor Kevin W. Plaxco, Chair

Professor Irene Chen

Professor Michael J. Mahan

June 2019

The thesis of Ava Shruti Kartik Greenwood is approved:

_____

Irene Chen

_____

Michael J. Mahan

_____

Kevin W. Plaxco, Committee Chair

June 2019

Exploring structural modifications and biomarkers to optimize and expand the E-DNA scaffold sensor for applications in point of care serology

ACKNOWLEDGEMENTS

Graduate school, unsurprisingly, has been a time of great personal growth for me. Going from the little undergraduate from a small island in the middle of the Pacific, to the relatively well-traveled independent scholar in California has been an eye-opening experience. Leaving the Big Island to further advance my education was always a dream of mine, one which graduate school at UC Santa Barbara allowed to come to fruition. But it was more than getting off the fiery volcanic rock: my experience has allowed my transition into an independent scientist and enabled me to form lasting relationships with people of similar intellectual backgrounds and personal interests.

To all of the post-doctoral researchers in the group: your teaching, support, assistance and pep talks throughout the years helped me continue in the face of adversity. To my fellow graduate students in the group: having someone to talk with about the struggles of graduate school and laugh about failed experiments was invaluable. To Kevin: thank you for your years of mentorship, guidance and friendship.

To all of my friends from graduate school: the lunch dates, the camaraderie, the crazy workouts, the coffee dates, the game nights, the concerts - all these things kept me happy and sane during the down times. Erin and Shelby, thank you for always motivating me to work out and hangout with my girlfriends, and for not giving up on me when I skipped the gym for weeks on end. Mahdi, Camden, Evan, and Brett, thanks for always being down to do something fun and a little wild, if only to remind ourselves that we have a life outside of graduate school.

To my family who viewed my tenure in graduate school as the achievement of a lifetime: Mommy Ami, Mattie Rel, Bluet, Dad, Bubby and Peter. Your unending support and

belief in me, after the significant trials and tribulations in our lives, kept me going at even the worst of times. There was nothing like escaping back home to work in the garden digging turmeric or surfing. Living in California allowed me spend holidays mainland family, and I realized that while nieces are super cute, I do indeed dislike snow and the cold. Through visits and frequent phone calls, you've reminded me of the life I love outside of graduate school.

And Chris, where to even begin? My rock, my safe place, my favorite human, my greatest supporter, my greatest motivator, my workout monster. Nothing I become would be possible without you or your support. The late night kombucha runs, the disapproving looks when I skipped a workout, the eyerolls when I complained about life, you withstood it all with a smile and your unruffled personality like a champ. Don't ever change, unless you get even faster.

ABSTRACT

Exploring structural modifications and biomarkers to optimize and expand the E-DNA scaffold sensor for applications in point of care serology

By

Ava Shruti Kartik Greenwood

Serology provides comprehensive information about infection, disease progression, and immune history. Current technologies utilized for serological diagnosis exist in one of the following modalities: 1) rapid, qualitative and easy to use in complex clinical samples, but limited to a single diagnostic biomolecule, 2) cutting edge and quantitative but computationally expensive and unable to perform well in complex clinical samples, or 3) quantitative, robust and easily multiplexed using complex samples while being time and equipment intensive. To bridge the gap between rapid and qualitative and time/equipment intensive and quantitative, our group has developed electrochemical DNA (E-DNA) scaffold sensors to quantitively detect diagnostic antibodies in a rapid, single step, wash free, electrochemical system. The overreaching goal is to develop an inexpensive, multiplexed E-DNA scaffold sensor to detect multiple diagnostic antibodies at the point of care in less than 15 minutes – which will improve patient outcomes and reduce the number of patients lost to follow-up.

The work presented here focuses on improving the analytical and clinical performance of the E-DNA scaffold sensors, in addition to expanding the platform to diagnose multiple sexually transmitted infections. Compared to the scaffold sensor structure in previously published literature, various modifications of the scaffold sensor flexibility and

utilization of a bivalent epitope probe did not improve the overall current, signal gain, or limit of detection of the E-DNA scaffold sensor. Attempts at expanding the E-DNA scaffold sensor to detect anti-gp41 diagnostic antibody in clinical samples resulted in a successful sensor that approaches the sensitivity and selectivity necessary clinical utilization, however incorporation of two linear epitopes of herpes simplex virus type 2 and hepatitis C were unsuccessful with the linear epitopes employed. Difficulties in expanding the diagnostic biomarkers utilized in this platform stem from issues incorporating linear immunodominant epitopes, which demonstrate positive and negative predictive value when challenged with human sera using gold standard techniques yet demonstrate no significant signal change when incorporated into the E-DNA scaffold.

TABLE OF CONTENTS

LIST OF FIGURES

Chapter 1. Introduction

1.1 Serology at the point of care

Blood and blood products, such as serum and plasma, contain molecular biomarkers that can provide us with a unique and unparalleled view of metabolism, infection, auto-immune disease, oncology, and a patient's response to treatment[1–3]. Thus motivated, serology is the study of the protein, cellular and metabolic components of the blood to gain meaningful insight into an individual's current health. Use of serology typically occurs during a patient's visit to a physician for diagnostic or wellness purposes, where in blood is drawn and relevant studies are performed to provide the medical practitioner with an in depth look into the biology behind a patient's symptoms.

The 21st century is rapidly becoming characterized by the ease and speed with which we can accomplish most tasks, and yet obtaining meaningful, actionable health related results is still a slow and cumbersome process. In the typical primary care provider-patient interaction, one must make an appointment to discuss their symptoms and undergo a physical exam, where the provider listens to a medical history of the ailment and orders a number of serological tests for diagnostic purposes. Unless one is in a hospital (such as emergency department), patients are typically referred to an off-site, centralized facility to have their blood taken by a phlebotomist[4]. There, the sample is either tested by a technician with specialized training and equipment or sent to a centralized facility that performs these tests regularly. In addition to the time required to draw blood and transport it to a facility appropriately equipped to carry out the diagnostic tests of interest, most serological diagnostic tests are likewise slow as they are multistep and require long incubation times[3,5–7]. If we evaluate this timeline, we see that the lag

between a patient-physician interaction and the time the physician receives actionable diagnostic information ranges from hours (if testing is performed in a hospital) to days (if the sample needs to be collected separately and processed at a separate, centralized facility)[8,9]. Clearly there is room for improvement in the current, laboratory-centric approach to the measurement of molecular markers.

Given that a typical patient-physician interaction lasts approximately 15 minutes[10], it would be useful to develop serological tests that can provide significant diagnostic information within this timeframe, such that health care providers can make informed decisions about patient care in a timely manner: at the "point of care." To aid (and focus) efforts to develop such technologies the World Health Organization has come up with a set of guidelines, ASSURED. The acronym relates the following conditions for the development of point of care diagnostic tests: affordable, sensitive, specific, user-friendly, robust and rapid, equipment free, deliverable to those who need them[2]. The development and subsequent use of point of care diagnostic testing has many benefits both in the developed and developing world: namely, it will increase the speed and frequency of detection and diagnosis, thus allowing providers to take appropriate steps to treat an identified ailment/disease in a single visit; reduce the number of patients who are lost to follow up; allow for enhanced screening and treatment in remote clinics and areas where routine healthcare is interrupted; and provide a means for epidemiological surveillance of disease in near real-time; all of which will lower the transmission of disease and contribute to improved patient outcomes.

Perhaps the most widespread and informative diagnostic biomarkers in use are antibodies. These Y-shaped proteins (for the immunoglobulin G class), produced by the

immune system in response to pathogens such as viruses, bacteria and fungi[11] or, sometimes, the body itself, consist of a constant region and a variable region. The variable region, which is located at the ends of the two arms of the Y, non-covalently binds to antibody's target molecule, called the antigen. The region on the antigen the antibody binds to can either be a contiguous amino acid sequence, called a linear epitope, or based on amino acid proximity in the native state of the antigen, called a conformational epitope. As the culmination of millions of years of evolution perfecting non-covalent binding events, antigen-antibody interactions are highly specific and highly selective[12].

1.2 Current point of care diagnostic techniques for detecting antibodies

While the appeal of point of care diagnostic testing has driven decades of research to achieve this end, there are currently only two types of tests that are being employed in the field: lateral flow immunoassays (LIAs) and agglutination assays. Both are utilized to detect diagnostic antigens or antibodies against a specific biomolecule as a means of diagnosing viral, bacterial, or fungal pathogens[3,13,14].

LIAs are small easily utilized serological devices, otherwise known as "dip-sticks," the most mainstream of which is the at home pregnancy test. A typical LIA utilizes a protein adsorption resistant membrane, such as cellulose, that utilizes capillary action to diffuse a serological sample of interest, such as blood or serum, through the membrane to a "test line" and a "control line"[15,16]. The conjugation pad, where the target biomolecule is bound by a reporter, typically utilizes a nanoparticle labeled biomolecule conjugate, with either a metal/carbon-based nanoparticle that elicits an observable color change or luminescent nanoparticles that can be interpreted optically[13]. The test line

consists of a primary biomolecule against the target analyte, whereas the control typically consists of a secondary biomolecule that recognizes a universally present target, typically an antibody against the constant region of human immunoglobulin G (IgG)[3,13,15,16] (*Figure 1*). As the sample diffuses through the conjugation pad, serological targets against the test (if present) and the control specifically and selectively bind with the labeled conjugate biomolecule. As they travel down the length of the LIA, they are then captured by the primary and secondary biomolecules. If the target molecule is present in a high enough concentration an observable signal indicative of that disease will appear within the few minutes afforded for a point of care device.

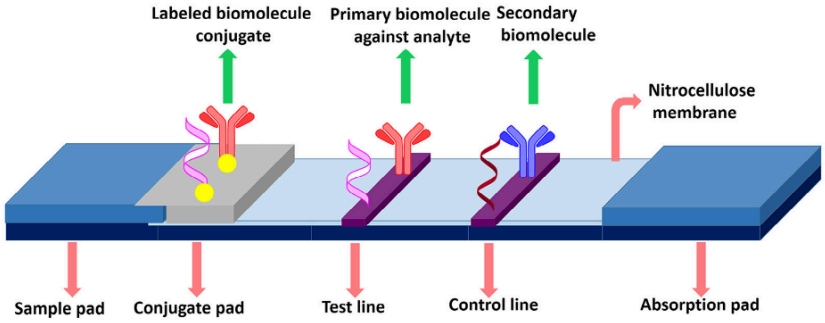

Figure 1: Schematic of lateral flow immunoassay. Small volumes (~20 uL) of unprocessed clinical samples (e.g. serum or blood) are added to the sample pad. Through capillary action the sample flows towards the absorption pad. The control biomarker and the target biomarker of interest, if present, conjugates with the biomolecule conjugate in the conjugation pad. They are then captured by the capture biomarkers on either the test or control lines. In high enough concentrations of the target biomolecule, accumulation of the labeled biomolecule conjugate yeilds a visible color change. Figure taken from Bahadir et al. 2016.

Agglutination assays utilize the ability of antibodies to clump together cells or particles in the presence of a target antigen. While agglutination occurs naturally in the body (hemagglutination), diagnostic tests utilizing this phenomenon have been developed by attaching diagnostic antibodies to latex beads[14]. In the presence of the target pathogen, which expresses the antigen of interest, the antibodies on multiple latex beads will bind to

a single pathogen, resulting in the formation of visually observable aggregate[14] (*Figure 2)*. However, the same limitations present for the LIA also exist here—results depend on a visual interpretation.

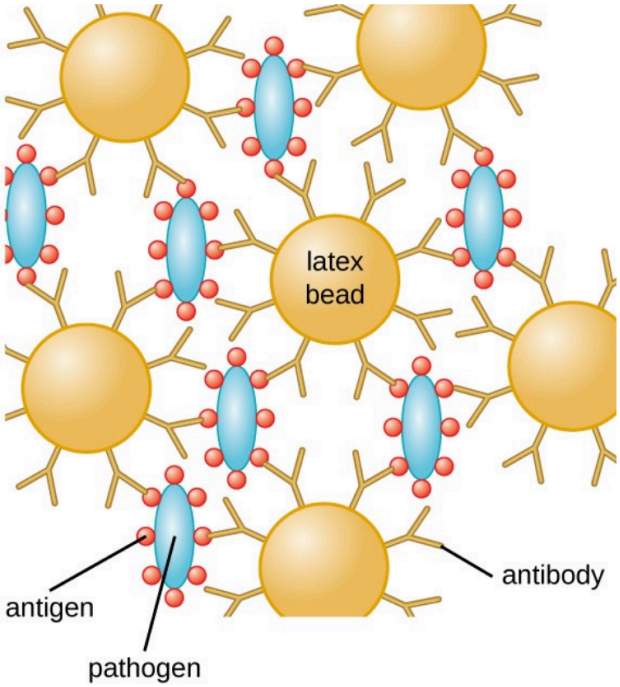

Figure 2: Agglutination assay in action. Latex beads conjugated with specific diagnostic antibodies recognize the pathogen of interest through highly specific antibody-antigen interactions. In the presence of multiple pathogens, the multiple latex bead antibody and pathogen antigen interactions cause visible clumping in the clinical sample. Figure taken from Ortega-Vinuesa et al., 2001.

In controlled environments, both LIAs and agglutination assays often achieve sensitivity and selectivity over 95%, but when utilized at the point of care performance diminishes significantly[13,15,17]. Further problems arise when these tests are utilized in the field, namely that false negatives or positives can be diagnosed due to method of reading the test—using the human eye. While easy to utilize and rapid, there are two inherent factors that affect the scope and implementation of these point of care diagnostic devices:

the inability to detect multiple targets in a single complex sample, and the necessity of a high antibody titer coupled with the absence of quantitative biomarker information.

Commercially available LIAs are limited to the detection of one specific biomolecule, and therefore, are only used to detect one disease. Limitations of the current LIA design, which make them able to only detect a single target biomolecule, stem from interference of different target biomolecules and difficulty tuning the spatial separation of test strips. These factors can only be resolved by larger sample volumes and longer test strips, which means longer wait times for diagnosis. Furthermore, introducing multiplexing to a LIA comes at the expense of simplicity and operability by untrained personnel[3]. Similarly, agglutination assays can only detect one target because complex samples contain diffuse pathogens and biomarkers, and one would not be able to determine if aggregation is the result of one or more targets. Attempts at creating a multiplexed agglutination test requires a complex microfluidic system, automated addition of patient samples, and computerized interpretation of array results[18]. Similar to LIA, this multiplexable agglutination assay comes at the cost of large patient sample volumes and diminishes the ease of use for personnel without specialized training and equipment. As of 2019, there is one commercially available LIA and no agglutination assays that meet the ASSURED criteria set by the WHO that detect multiple biomarkers and/or diseases[6,19,20].

Current commercially available point of care devices rely on a visually interpreted signal output in response to a relatively high diagnostic antibody concentration. The limits of detection for LIAs and agglutination assays are within the single nanomolar regime when performed in buffer in a laboratory environment[3,13], however when challenged with complex samples in the field they typically miss seroconversion of a

patient during the initial stages of infection. This is due to the necessity of a high antibody titer, which is the concentration of antibody that the body has generated against a specific target, relative to all other antibodies present. Quantifying the intensity of a color on the test line on a LIA or the size of the clump as a result of agglutination to determine target biomolecule concentration is inexact, especially when interpreting these results using the human eye. As a result, neither diagnostic platforms are able to provide quantifiable biomarker information. As a result of these limitations, these assays are typically utilized at the point of care for initial diagnosis, wherein a second sample is sent off for more comprehensive and robust testing in a laboratory[19].

1.3 Other techniques in development for point of care antibody diagnostics

Another method that is currently in development for point of care antibody diagnostics is the wash-free fluorescence polarization immunoassay (FPA). Polarized light is used to excite a fluorescent dye or label that is attached to a target molecule, causing a change in photon emission relative to the plane of polarization as a function of complex size[21]. A typical FPA utilizes a fluorescent tag covalently linked to an antigen, with a known fluorescence polarization that is directly dependent on the effective molecular size of the fluorophore-antigen conjugate. Upon binding of the target diagnostic antibody to the fluorophore-antigen conjugate, the effective molecular size drastically increases, resulting in a higher polarization of the emitted photon[22].

The results of the FPA are then compared to those of a standard curve of fluorescence polarization versus target antibody concentration, which yields a quantitative result as long as antibody concentration is within the limit of detection[22]. Unfortunately, the FPA typically results in a small observable change in signal, as low as

15%, with background fluorescence polarization from non-specific adsorption typically around 10%, indicating a net 5% signal change to inform for diagnosis. Because of this, considerable signal averaging, background subtraction, and large sample volume requirements limit the applications of this technique. Furthermore, this process is not easily multiplexed and requires the use of specialized equipment and has only been successfully utilized in well-equipped facilities[23].

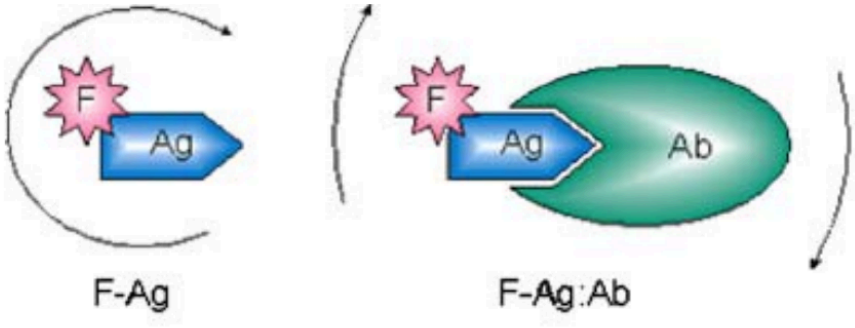

Figure 3: Schematic of the principle behind fluorescence polarization anisotropy. In the absence of target, the fluorophore-antigen pair emits a photon at a known angle relative to the angle excitation of plane polarized light. Binding of the antibody to the fluorophore-antigen pair drastically increases the effective size of the complex, and thus changes the angle of photon emission to the same polarized light. Figure above was taken from Smith et al. 2008.

Motivated by the need for improved point of care serological methods, a wide range of new molecular biosensors and techniques have emerged to fill this gap. Because most antibody-antigen binding events do not undergo a conformational change, they do not produce any easily measurable or observable signal[22,23]. As such, methods have been developed that monitor antibody-antigen binding via associated changes in adsorbed mass (e.g., quartz crystal microbalance)[24], optical properties (e.g., surface plasmon resonance)[25] or electric field (e.g., field effect transistors)[26]. Thus far, these techniques

perform well when challenged with purified antibodies in simple buffers in a research setting. All these methods are easily operated, sensitive, and provide quantitative diagnostic information, however, they fail when challenged with realistically complex clinical samples, such as serum or whole blood. This reduces the efficacy and application for these different molecular diagnostic techniques at the point of care, namely because, as previously mentioned, further dilution or equipment intensive sample processing is required to distinguish between the background signal from non-specific adsorption and binding of target antibody.

1.4 The gold standard diagnostic technique for detecting antibodies, ELISA

Juxtaposed with current and developing point of care diagnostic techniques, the enzyme linked immunosorbent assay (ELISA) provides a highly sensitive, highly selective platform for detecting diagnostic antibodies and antigens in small volumes of minimally processed clinical samples. ELISA was developed in the 1960s when it was discovered that protein adsorbed to a solid surface through hydrophobic interactions was still able to participate in high affinity binding events, like the binding between an antigen and specific antibody[27]. A typical ELISA immobilizes either the target antigen (direct ELISA) or antibody (capture/sandwich ELISA) to a hydrophobic surface, such as a 96-well polystyrene plate, followed by stringent washing with buffer containing detergent. The ELISA is then blocked with a non-reactive, ubiquitous protein like albumin to prevent any antibody adsorption or interactions not directly related to binding between the target antigen-antibody pair. After an additional wash to remove unabsorbed blocking protein, the ELISA is incubated with a small volume (~100 μL) of the sample of interest. Following target sample incubation, the ELISA is again stringently washed,

before the addition of a reporter antibody. Reporter antibodies are primary and secondary antibodies that are conjugated with a small molecule or protein, such as biotin or horseradish peroxidase. After another stringent washing step to remove unbound conjugate antigen, the enzyme and/or substrate of the antibody conjugate is added to ELISA, wherein the resultant chemical reaction yields an observable signal, typically colorimetric[28]. These results are then interpreted using a spectrophotometer, where absorbance at a given wavelength is directly proportional to the concentration of antibody/antigen target in the sample[27,28].

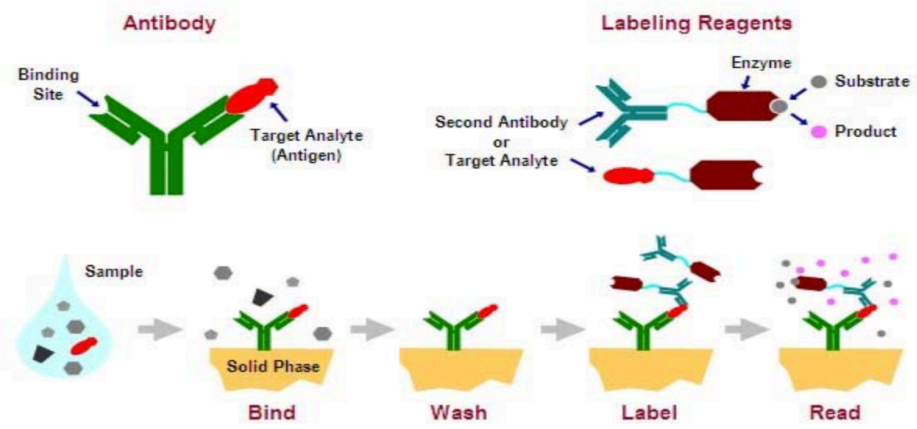

Figure 4: Schematic of ELISA. Target biomolecule in the complex clinical sample interacts with the capture biomolecule (either antigen or antibody) which is immobilized on the solid phase. Unbound components of the sample are washed away. Secondary antibody with an enzyme reporter then binds the target biomolecule, with unbound secondary antibody washed away vigorously. Enzyme reporter substrate is then added and then the colorimetric signal change is read using a spectrophotometer. Figure taken from Carvalho et. al 2014.

The application and utility of ELISA is extensive as it is easily multiplexed, highly sensitive and quantitative, and has a high signal to noise ratio. Firstly, due to the typical schematic of ELISA plates, multiple antigen-antibody pairs can be detected simultaneously against several different clinical samples with small variations in well-to-well protocol. Second, because of the signal amplification that occurs with the reporter-

antibody conjugate, the limit of detection for diagnostically significant antibodies can be within picomolar concentrations. Lastly, as the result of high-fidelity antigen-antibody binding, signal amplification, blocking to prevent non-specific adsorption, and extensive washing steps, complex clinical samples can be utilized in this diagnostic technique with excellent signal to noise. Because of these attributes, ELISA is currently the gold standard for immunodetection for most diseases[6,19,29].

Despite these positive attributes, ELISA is a laboratory intensive diagnostic technique that requires highly specialized technicians, well equipped facilities, expensive equipment for analysis, and most importantly, time. Each of the multiple steps of ELISA requires optimization: from buffer pH, to blocking and detergent concentrations in buffers, to serum dilutions to prevent signal saturation, to secondary protein conjugated-antibody concentrations. Also, because of the numerous steps involved in ELISA and the high sensitivity, the potential for human error or contamination resulting in a false positive or negative result is high. As a result, highly trained technicians (or in a centralized facility, automated robots) with well established, clean workspaces are a requisite of successful ELISA experiments[27,28]. Furthermore, the standard instrument used for analyzing either the colorimetric or fluorescent results of ELISA, the Tecan Microplate Reader, is bulky and has a cost within the thousands of dollars. Lastly, as the result of multiple incubation and washing steps, the typical ELISA takes approximately four hours to complete at minimum if performed continuously[30].

1.5 Electrochemistry to detect diagnostic antibodies at the point of care

As we previously described, current and even developing point of care diagnostic tests struggle to provide quantitative actionable diagnostic information and increase the

signal to noise ratio, while maintaining the high sensitivity, selectivity and multiplexing provided by the laboratory-bound gold standard ELISA. The development of electrochemical DNA (E-DNA) scaffold sensors may provide a solution to bridge the gap between current deficits in point of care technologies and laboratory approaches: providing a rapid, single step, quantitative, easily multiplexed platform for the measurement of specific antibodies[17,31].

Currently, E-DNA scaffold sensors are fabricated on a gold electrode surface that has been rigorously cleaned and etched through a series of oxidative and reductive steps. Taking advantage of the well understood gold-thiol chemistry[32], a single stranded DNA molecule with a terminal (5') reduced sulfur and a distal (3') redox reporter (e.g., methylene blue or ferrocene) can be covalently attached to the gold surface[17,31,33]. After functionalization of our reporter strand, an anti-fouling self-assembled monolayer with a terminal thiol (e.g., mercaptohexanol, mercaptodecanol, biometric phospatidylcholine) is then used to back-fill the electrode, binding to the unoccupied gold on the electrode surface[34]. Finally, the DNA molecule is hybridized with a complementary peptide nucleic acid sequence (PNA) with a distal linear epitope which has been demonstrated (in peer-reviewed experimental literature) to bind diagnostically-relevant antibodies. Once the E-DNA sensor is fabricated, all that is required is to submerge the electrode in a small volume of an unprocessed clinical sample (e.g. 200 uL) in a single step and for a definitive positive or negative result. In the absence of the target antibody, the DNA-PNA scaffold allows the redox reporter to approach the electrode surface and exchange electrons when potential is applied in a window surrounding the reduction potential of the reporter. In the presence of target antibody, the non-covalent binding of the relatively

massive, heavy antibody (~150 kDa) to the epitope reduces the ability of the redox reporter to approach the electrode surface, which results in a decrease in current[17,31,35] (*Figure 5)*.

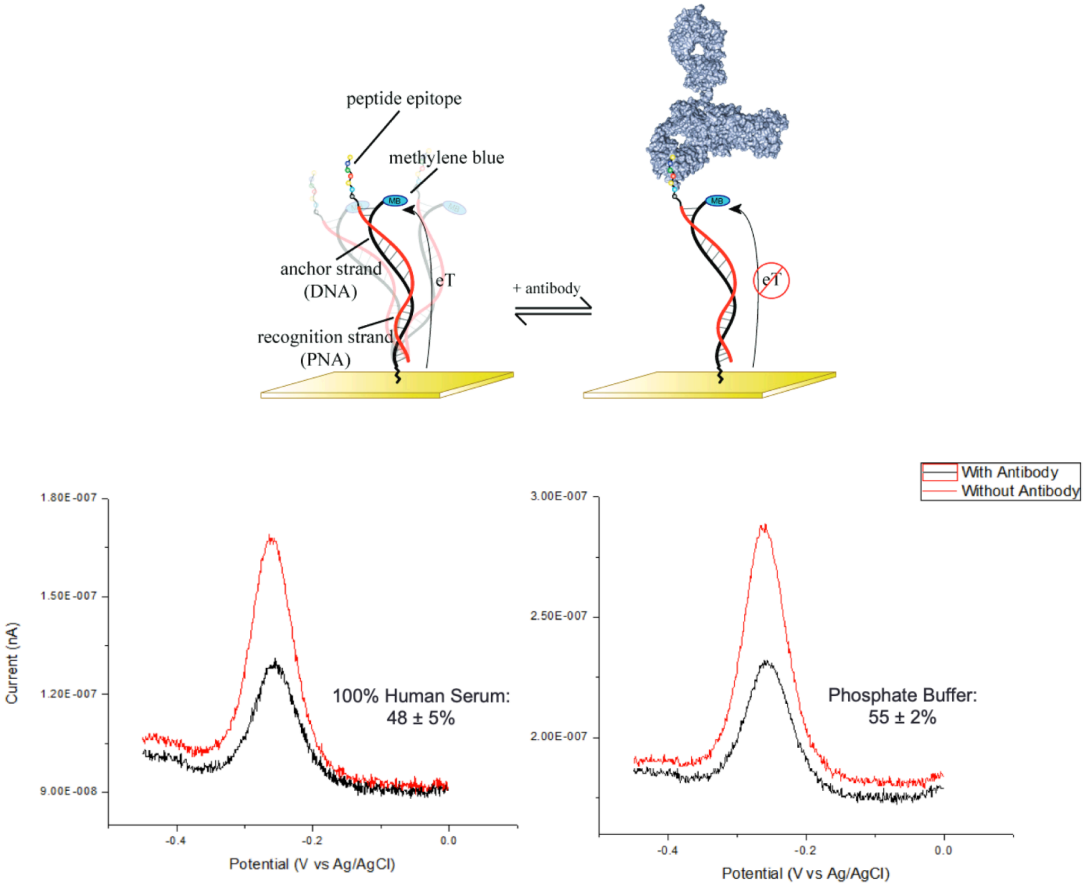

Figure 5: The E-DNA scaffold sensor in action. (Top) From left, the E-DNA scaffold built on the electrode surface before addition of the complex clinical sample. The DNA anchor strand with terminal redox reporter (methylene blue) is covalently linked to the gold electrode surface. A complementary PNA with a distal linear epitope hydrogen binds through nucleobases. In the absence of target antibody, this DNA-PNA approaches the electrode surface and the redox reporter is able to exchange electrodes. Upon addition of target, the binding of the large antibody to the relatively small DNA-PNA scaffold reduces its' ability to approach the electrode surface, reducing the electron exchange between the gold surface and the redox reporter (Upper figure portion taken from White et al. 2012). (Bottom) The response (change in current) of the E-DNA scaffold sensor in the presence (black) and absence (red) of antibody as a function of potential. The response of the sensor in 100% serum and buffer is 48± 5% and 55± 2%, respectively.

E-DNA scaffold sensors allow for rapid detection in two ways, 1) because we are measuring the sub-second electrochemical reaction of our redox reporter, and 2) the

binding of an antibody to its target epitope typically reaches equilibrium within a matter of minutes[12,17]. Typically, the signal gain by the sensor in response to the diagnostic antibody of interest in a positive unprocessed clinical sample ranges from 25-50%, whereas the background signal from non-specific adsorption of molecules in a negative, but similarly unprocessed clinical sample ranges from 8-15%[17,36,37]. This is due to the physical properties of the sensor; in addition to the anti-fouling monolayer, non-specific binding of other antibodies, serum proteins, platelets, and cells do not alter the dynamic interaction and electron transfer between the redox reporters in the sensor population and the electrode surface[12,38,39].

Through characterization of the E-DNA scaffold we are also able to obtain information regarding the limit of detection, the dissociation constant (K_D), and determine antibody titer. In a paper published in our group by White and collaborators in 2012, five E-DNA scaffold sensors were designed to detect antibodies indicative of the human immunodeficiency virus. When challenged, these sensors rapidly, specifically and selectively recognized their target antibodies at sub-nanomolar concentrations with K_Ds in the single digit nanomolar range, which is within the range of clinically relevant antibody concentrations[17]. Further development of one of these E-DNA scaffold sensors against the HIV envelope glycoprotein 41 (gp41) in our group by Patterson and collaborators was able to detect the antibody titer of a clinical sample, showed excellent agreement with commercially available recombinant immunoblot assay (RIBA), while out-performing the limit of detection for a commercially available LIA[40].

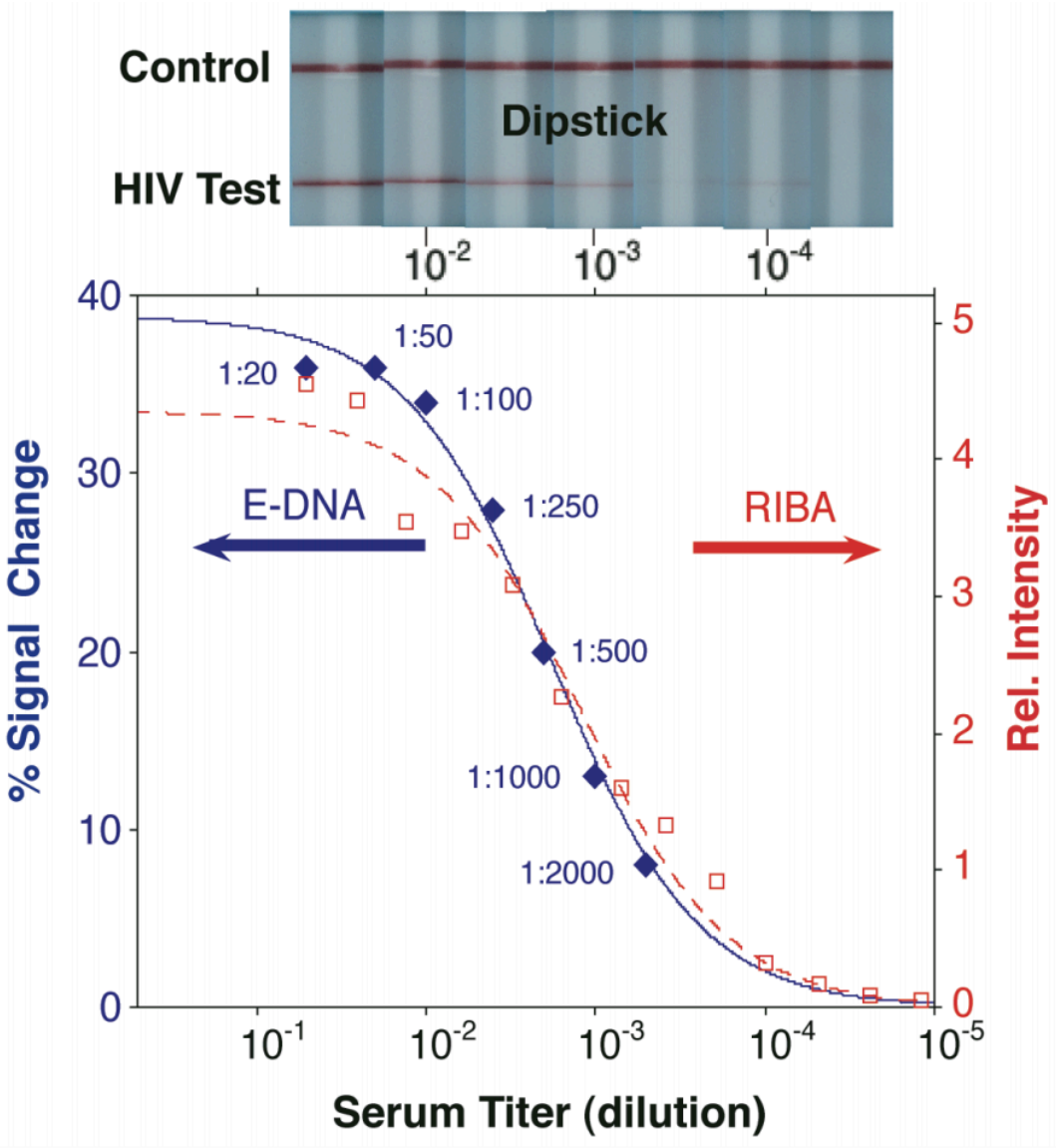

Figure 6: Quantitative determination of the serum titer in a HIV positive clinical sample using the anti-gp41 E-DNA scaffold sensor (blue) as compared to commercially available LIA (top) and gp41 RIBA (red). While the LIA fails to detect dilute concentrations of the diagnostic gp41 antibody, the E-DNA scaffold sensor determination of serum titer closely matches the determination of serum titer of the commercially available anti-gp41 RIBA up to a two-thousand-fold serum dilution. Figure taken from Patterson et. al., unpublished.

Multiplexing with E-DNA scaffold sensor can be accomplished with relative ease. Using lithography, electrodeposition, or wet chemistry, electrodes can be fabricated into a microarray to simultaneously detect multiple diagnostic antibodies and with positive and

negative controls[31,41]. In the academic setting, fabrication of these multiplexing microarrays becomes tedious and expensive, and hand-fabrication unfortunately promotes sensor to sensor variation and limits the compactness of the array, increasing requisite sample volumes. However, large scale production of these sensors using robotic microarray contact printers and a Biodot array printer will resolve these issues. With automation and the availability of portable, inexpensive, easy to use potentiostats[42], this technology can be utilized at the point of care. This technology can be expanded to multiple different disease targets and serological markers in one, chip like device that would allow for multiplexed detection of multiple diseases in a small sample volume (~100 uL). Furthermore, automated fabrication of E-DNA sensors is inexpensive, with each sensor costing approximately $2US.

1.6 Sexually transmitted infections and justification for use as our test bed

As our test bed for validation of the E-DNA scaffold sensor, we have focused on the detection of antibodies diagnostic of sexually transmitted infections (STIs). Our reasoning is three-fold, 1) there exists a broad modality of infection and disease states, 2) STIs are extremely prevalent, well studied and development of a point of care diagnostic technology has high impact, and 3) because human samples, antibodies, and well established diagnostic immune tests are readily available.

Sexually transmitted infections result from two types of pathogens, either bacterial or viral. Bacterial STIs include gonorrhea, chlamydia and syphilis, are curable with an appropriate course of medication. Viral infections include HIV, herpes simplex virus 1 (HSV-1), herpes simplex virus type 2 (HSV-2), hepatitis A virus (HAV), hepatitis B virus (HBV), hepatitis C virus (HCV), and human papillomavirus (HPV)—most of

which are incurable but for which treatment and management exists. During the course of infection, whether curable or incurable, antibodies are generated against the pathogen. Analysis of the immune history of a patient by detecting specific antibodies not only provides information about current infection but can provide information about past exposure and immunization history.

According to the World Health Organization, an estimated 499 million new cases of curable STIs occur every year, an estimated 536 million people are estimated to be living with incurable HSV-2, and 219 million women are living with HPV[43]. Because of the large number of people from different regions and demographics affected by STIs, they have become the subject of extensive research and study. Comprehensive research exists on the structure and clinical course of these diseases, and extensive mapping of epitope mapping has been performed to aid in the development of diagnostic serological assays. In developed countries, such as the USA, screening for STIs is limited due to testing ease. For example, the Center for Disease Control reports that although 82% of women aged 15-24 that are sexually active receive contraceptive or STI testing, only 39% receive both[44]. Furthermore, only 27% of women seeking emergency contraception were screened for STIs, with 12% of them testing positive for at least one[45]. In developing countries, STIs are found with even higher frequency as a result of limited access to health care, diagnostic devices, and thus treatment. As such, there exists a need for rapid, uncomplicated diagnostic tests that can be performed with minimal, inexpensive equipment at the point of care to inform patients, improve outcomes and for easier epidemiological surveillance.

Here, we will take advantage of the prevalence and extensive study of STIs to develop our E-DNA scaffold sensor against high impact targets. Because of STI prevalence, authentic human samples indicative of a specific disease stage (acute infection, chronic infection, past exposure, immunized) from commercial vendors for research purposes is easily accessible. Furthermore, there are many vendors offering monoclonal and polyclonal antibodies against STIs for use as controls and or to determine limits of detection. Lastly, extensive immunodetection assays, such as ELISA and LIA, against a wide variety of antigen and antibody targets are available commercially. Many of these tests have undergone rigorous analysis by organizations such as the WHO and are recommended in the STI guidelines as the diagnostic standards for point of care and laboratory-based methods[6,19,43].

1.7 Internal controls for point of care E-DNA scaffold sensors

FLAG is a linear sequence of amino acids (DYKDDDDK) specifically developed for immunoaffinity chromatography. Because of its sequence, it does not interfere with the native folding of proteins, is water soluble and has a built in enterokinase-cleavage site for removal following protein purification. Furthermore, several monoclonal antibodies that bind flag have been raised, the most promising of which is the anti-flag monoclonal antibody M2, which is able to specifically and selectively bind the epitope in conditions mimicking biological environments (pH 7.6) without the presence of bivalent cations[46]. Because of its widespread use in immunochromatography, monoclonal antibodies against FLAG are readily available.

Given the above, FLAG would work as an excellent internal control for our E-DNA scaffold platform. Previous work has demonstrated, incorporating the FLAG epitope into our

E-DNA scaffold sensor architecture results in a signal change of ~50% when challenged with saturating concentrations of monoclonal antibody[17]. Furthermore, because this is an artificial epitope, there is minimal chance of antibodies present in human clinical samples cross reacting to give false positives[17].

Chapter 2: Structural modifications of the DNA-PNA Scaffold to improve analytical performance

2.1 The current performance of the E-DNA scaffold sensor

As previously shown, the E-DNA scaffold sensor is able to detect diagnostically relevant antibodies in unprocessed clinical samples to provide actionable results at the point of care. White and colleagues demonstrated that five of the developed e-DNA scaffold sensors demonstrate a signal change of ~45% in response to a specific target antibody, in buffer and in complex clinical samples. However, while being able to sensitively and selectively detect target antibodies in a sub 15-minute time frame[17], the result for the E-DNA scaffold sensor-antibody binding event is signal off, with a current change within the microamps. These sensors, while being able to detect clinically relevant concentrations of antibodies, would benefit from an increased limit of detection because it will decrease the time between infection and detection and improve the positive and negative predictive value of the test[43]. Thus, one of the first goals to improve the E-DNA scaffold sensor platform is to optimize two things: overall current and change in signal upon binding of the target antibody, and to improve the limit of detection.

2.2 Structural modifications of the DNA-PNA scaffold to improve raw current and analytical sensitivity

While the mechanism of binding induced signal change by the E-DNA scaffold sensor is unknown, our group suspects this is due to a specific geometry of the antibody-sensor complex. While this complex has not been visualized, from a bioengineering perspective we can experimentally modify this geometry and evaluate the potential to improve the raw current of the sensor and the binding induced signal change.

The signal observed from E-DNA scaffold sensors is the result of a reduction of probability that the redox reporter will approach the surface on the electrode. Specifically, the current we observe as we scan the potential window surrounding the redox potential of our reporter is the population of sensor molecules able to approach the electrode surface and exchange electrons[47]. Upon binding of the comparatively large antibody to the E-DNA scaffold sensor, the probability that a redox reporter will approach the surface and thus exchange electrons is diminished, which we observe as a reduction in current. Because of this, we decided to utilize a voltammetric approach that is sensitive to changes in electron transfer kinetics, called square wave voltammetry. By slowing down the frequency of the potential applied to the system, we interrogate processes with a slower electron transfer rate with more sensitivity. While some DNA based electrochemical sensors are able to switch modalities from signal-on to signal-on by altering the frequency pulse, interrogation of the E-DNA scaffold sensor with a frequency pulse between 1 and 10,000 Hz was unable to induce signal-on behavior[17,48]. Because electron transfer kinetics of the rigid E-DNA scaffold in the absence of antibodies is already a relatively slow process, high-gain signal-on behavior is believed to be possible when interrogating the sensor with frequencies below 1 Hz, where the signal to noise ratio is too low to provide reliable results. However, we are still able to observe signal-off behavior in the microamps with appreciable signal to noise when interrogating the electron transfer rate with slower frequencies between 5 and 120 Hz.

To further improve electron transfer kinetics, thus increasing overall current and binding induced signal gain, we evaluated the effect geometric modifications of the sensor architecture and placement of the epitope relative to the redox reporter. As previously described, the E-DNA scaffold sensor consists of a double-stranded scaffold that is

completely complementarity. Because of this, the scaffold sensor duplex is assumed to be relatively rigid, even in the absence of target antibody, which one can assume reduces the ability for the redox reporter to approach the gold surface[35]. Furthermore, on both the reporter strand and the recognition strand, the attachment is made at the distal end, furthest from the electrode surface. While placement of the redox reporter has been shown not to significantly affect the electron transfer rates of a sensor duplex[49], modifications in complementarity that increase the flexibility of the scaffold, or decreasing steric effects on the redox reporter by moving the antibody binding site, may increase the electron transfer kinetics and thus raw signal. Because of this, we designed and subsequently evaluated several scaffold sensors employing a variety of base pair mismatches.

Due to cost (purchasing PNAs is in the thousands of dollars), DNA-DNA scaffold sensors were utilized to test this hypothesis. Utilizing the same 27mer DNA anchor strand with a distally attached methylene blue redox reporter, DNA strands with variable complementarity with a covalently linked immunogenic small molecule, digoxigenin, were used. As a negative control, we used the FLAG epitope displaying PNA. The first complementary sequence was a single stranded 27-base DNA with a distally linked digoxigenin that was completely complementary (Dig 1), which emulated the structure of previously published DNA-PNA scaffold sensor[17]. The second sequence was 27-base strand which employed a three base pair mismatch in the center of the construct with a distal digoxigenin (Dig 2). The third sequence was a 27-base strand with a distal digoxigenin containing a three base pair mismatch, followed by three complementary base pairs, followed by a second set of three mismatched base pairs, for a total of six base pair mismatches which were focused around the center of the construct (Dig 3). The fourth construct was a 10-base

strand with a distal digoxigenin that was complementary to the final ten residues of the anchor strand (Dig 4).

After mechanical and electrochemical cleaning of the electrode, the sensor was built on the surface using previously established protocols[17]. In short, 25 nM of DNA anchor in phosphate buffered saline was allowed to functionalize on the electrode surface for one hour at room temperature. This was followed by an overnight functionalization of a 6-mercaptohexanol SAM in phosphate buffered saline at 4°C. The following morning, the electrode was submerged in the 200 nM of the appropriate digoxigenin conjugated DNA in phosphate buffered saline for two hours at room temperature to allow the DNA strands to anneal.

As one of our goals was to determine if changes in complementarity, and thus flexibility, of the scaffold sensor affected the raw signal output, the signal (raw current) after annealing of the DNA complement was evaluated. This was accomplished by scanning the electrodes with differing complement constructs in triplicate, using square wave voltammetry (frequency of 60 Hz, amplitude 25 mA[17,40]) in 3x phosphate buffered saline after 20 minutes equilibration (*Figure 7*). From the figure we see that compared to the FLAG scaffold sensor and the other digoxigenin constructs, the Dig 4 construct nearly doubles the raw current. Unfortunately, based on these results, we see that even with these changes in complementarity of the sensor, the raw current observed is still within the microamp range, which is not a sufficient improvement over the currently utilized sensor architecture.

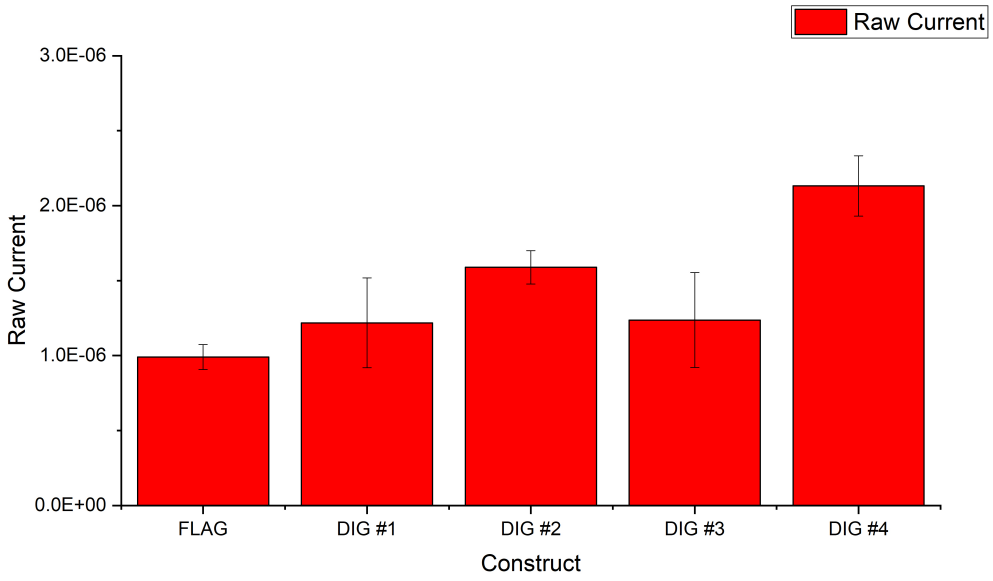

Figure 7: The effects of increased scaffold sensor flexibility on raw current. As seen above, while the shorter Dig 4 construct nearly doubles the raw current from the fully complementary Dig 1, the signal is still within the microamp regime, which is not a significant improvement over the current working construct. Data points are comprised of an average and the error bars represent the standard error (n=3).

After evaluation of the raw current as affected by changes in scaffold complementarity, the electrodes were immediately challenged with a saturating concentration of anti-digoxigenin monoclonal antibody, spiked into the 3x phosphate buffered saline to a final concentration of 30 nM. These electrodes were then scanned every 15 minutes over the course of an hour (*Figure 8*). As anticipated, the FLAG scaffold sensor showed no response outside of expected drift (4%), and the Dig 1 construct showed a signal change of 35%, which is within the realm of expectation for our antibody-scaffold sensor binding. However, modifications in sensor architecture by introducing base pair mismatches demonstrated a negative effect on signal gain. From the results we see that even the best performing of the base pair mismatch constructs, Dig 2, still underperformed the traditional sensor architecture by 10%.

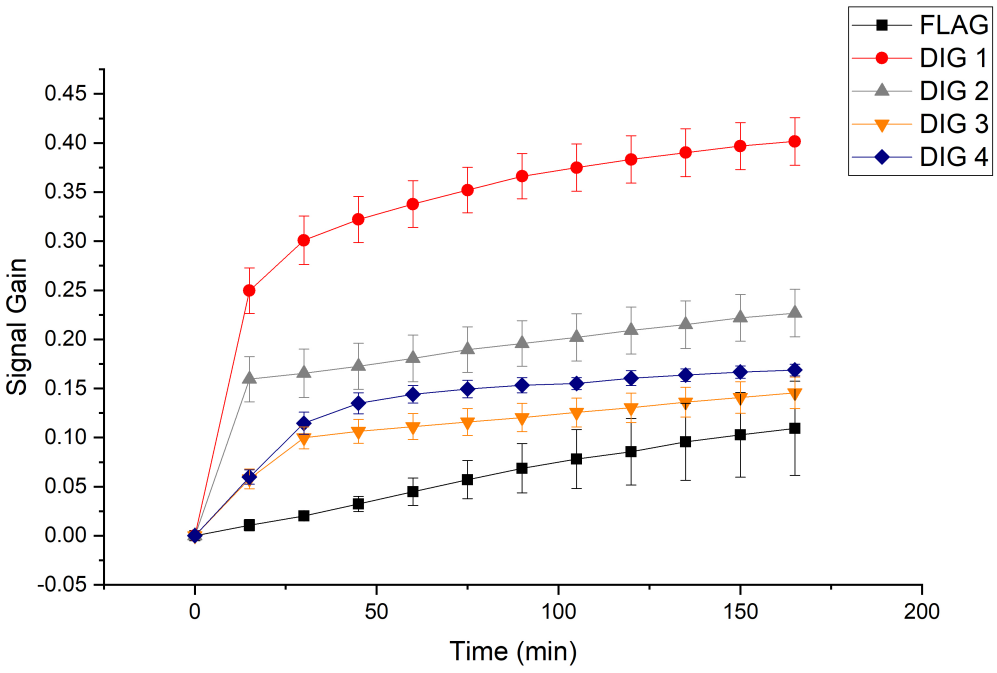

Figure 8: The effects of increased scaffold sensor flexibility on signal gain. The figure above illustrates signal gain as a function of time in the presence of 30 nM anti-digoxigenin monoclonal antibody for the four dig constructs of variable complementarity displaying a distal digoxigenin. As seen above, the completely complementary scaffold, with no bp mismatches, undergoes the largest signal change in response to saturating concentrations of anti-digoxigenin monoclonal antibody. The FLAG E-DNA scaffold sensor was used here as a control. Data points are comprised of an average and the error bars are the standard error (n=3).

2.3 Use of a bivalent epitope in the E-DNA scaffold sensor to improve analytical sensitivity

While our E-DNA scaffold sensor has shown to be able to detect diagnostically significant concentrations of antibodies in complex clinical samples, improving the limits of detection will allow for earlier diagnosis and subsequently improved patient outcomes. Previously published results using the E-DNA scaffold sensor employ only a single covalently linked linear epitope[17,31,40]. However, the structure of an antibody has two antigen binding domains which are spaced approximately 11.7 to 13.4 nm apart, where the epitope distance range is dependent on inherent flexibility in the antibody structure[50]. Taking

advantage of these two antibody binding sites could improve the sensor's affinity for its target, lowering its limit of detection.

In response to the above, an E-DNA scaffold sensor was designed with two linear epitopes presented on a single strand. Based on the distance between the antigen recognition sites, two PNAs presenting the FLAG linear epitope were designed with 10 base pairs complementarity to a DNA anchor strand, spaced approximately 12 nm apart. Due to the reduced number of DNA base pairs used to form the DNA-PNA duplex, the GC content of the duplex was raised to 70%, as opposed to the 26% used in previously published scaffold sensors[17], to increase the number of hydrogen bonds and thus increase of the stability of the DNA-PNA duplexes upon binding of the target antibody.

The bivalent epitope sensor was built on electrode surface using the same electrode preparation described in the section above, except the DNA anchor for the control and the bivalent FLAG sensor was annealed with 400 nM of PNA rather than of 200 nM, taking into account a doubling of number of duplexes on the DNA molecule. The electrodes were then placed into 3x phosphate buffered saline, where they were allowed to equilibrate for 20 minutes before being challenged with 60 nM of anti-FLAG monoclonal antibody, a concentration well above saturating. The sensor response to antibody was measured again at 60 Hz with an amplitude of 25 mV. However, the bivalent epitope (bivalent flag) performed very poorly when compared to the original sensor architecture (monovalent flag), demonstrating a 4% signal change versus 26% signal change in 15 minutes point of care window (*Figure 9*).

The main advantage that we hoped to gain by creating a bivalent epitope sensor was improved detection limits, ideally in complex samples. This was tested by challenging the

bivalent and monovalent epitope FLAG scaffold sensors with 5 nM of anti-FLAG monoclonal antibody under two conditions, one being 3x phosphate buffered saline, and the other being 3x phosphate buffered saline spiked with normal human serum to a concentration of 10%. After allowing the sensors to equilibrate in their electrochemical cells for 20 minutes to adequately remove any background signal from nonspecific adsorption, the sensors were scanned every five minutes for one hour following the addition of 5 nM anti-FLAG monoclonal antibody. As seen in *Figure 10*, while there is no appreciable response to the anti-FLAG antibody within our previously defined point of care window, the monovalent FLAG sensor in both the phosphate buffered saline and 10% human serum undergoes an appreciable signal change (~30%) in one hour. In comparison, the bivalent FLAG sensor only undergoes a 10% change in signal in the same amount of time.

The two most plausible reasons for the failure of the bivalent epitope sensor stem from either an ineffective architectural design of the scaffold, or changes in electron transfer rate, which means the new sensor requires optimization of the electrochemical interrogation parameters. The two main parameters that affect square wave voltammetry, and thus sensor gain upon binding of the target antibody, are frequency and amplitude. Using these two parameters, we can "tune" the electrochemical interrogation to optimize the signal gain of our sensors[48]. This said, we find that frequencies below 5 Hz produce poor signal to noise and that, because the transfer rate is relatively slow, frequencies above 500 Hz produce very little gain; thus we limited the frequency of our potential pulse between 5 and 500 Hz. Similarly, because amplitudes below 10 mV produce poor signal to noise and amplitudes above 100 mV cause substantial peak widening, we limited our amplitude investigation to this range. As we can see in *Figure 11*, within the range of electrochemical conditions that

work best for this sensor type[48], at saturating concentrations of monoclonal antibody the monovalent FLAG sensor (a) outperforms the bivalent FLAG sensor (b) by 30%.

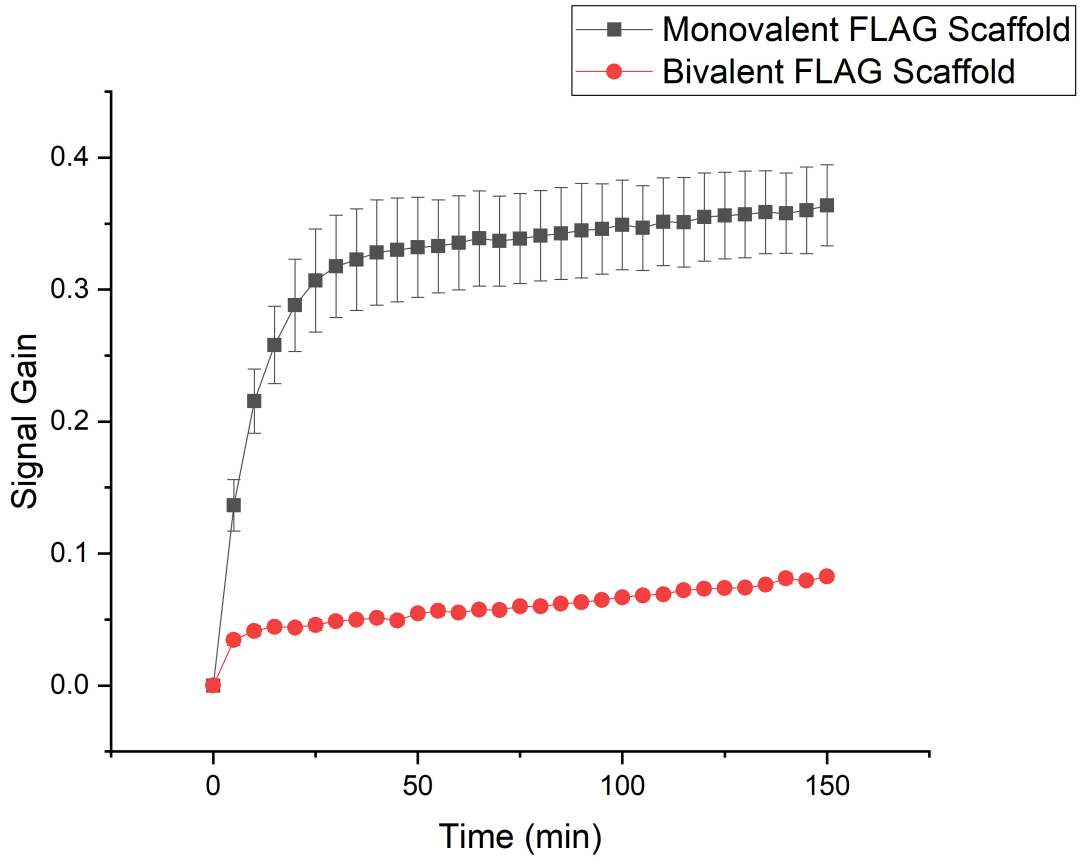

Figure 9: Performance of the bivalent epitope sensor in the presence of saturating target monoclonal antibody concentration. Bivalent FLAG epitope sensor is challenged with saturating concentrations (30 nM) of anti-FLAG monoclonal antibody with the monovalent FLAG epitope sensor as a control. As illustrated in the figure, the distal display of the monovalent FLAG epitope with completely complementary PNA significantly outperforms the bivalent FLAG epitope sensor with ten base pair complementarity, undergoing a signal change of 26% and 5% in fifteen minutes, respectively. Data points are comprised of an average and the error bars are the standard error (n=3).

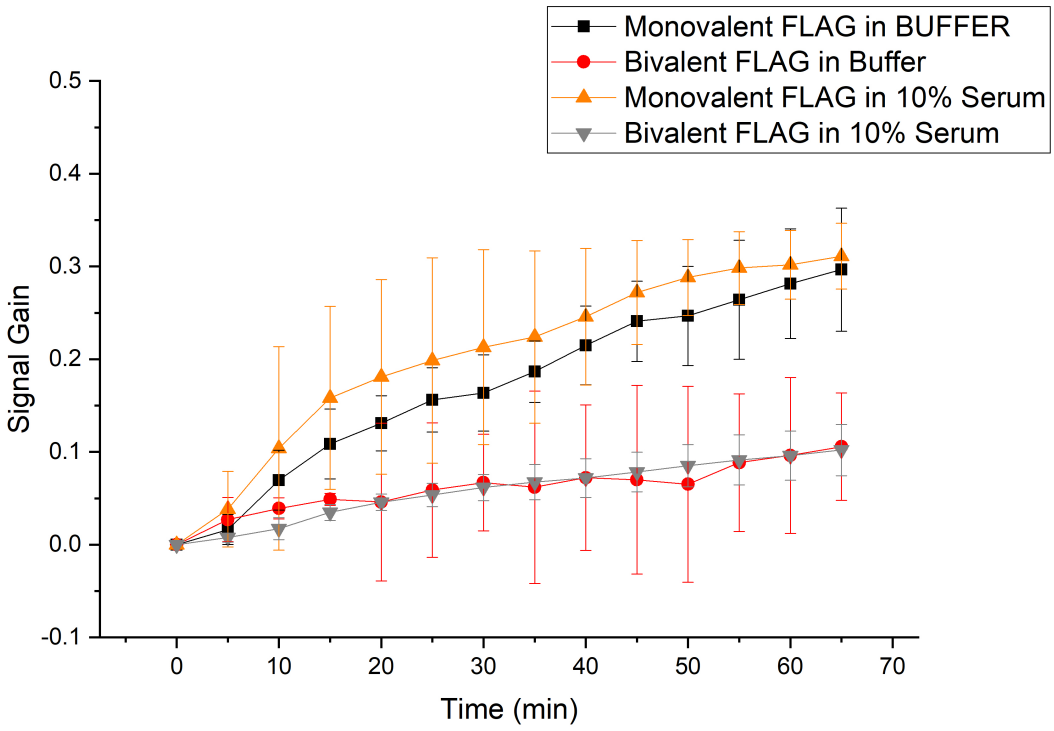

Figure 10: Performance of the bivalent epitope antibody sensor in the presence of low target antibody concentration. As indicated by the figure, bivalent epitope probes also do not improve the detection of antibodies at low concentrations. In buffer and 10% serum in the presence of 5 nM anti-FLAG monoclonal antibody, the monovalent FLAG epitope scaffold sensor outperforms the bivalent FLAG epitope scaffold sensor, undergoing a signal change of 30% compared to a signal change of 10% over the course of an hour. Data points are comprised of an average and the error bars are the standard error (n=3).

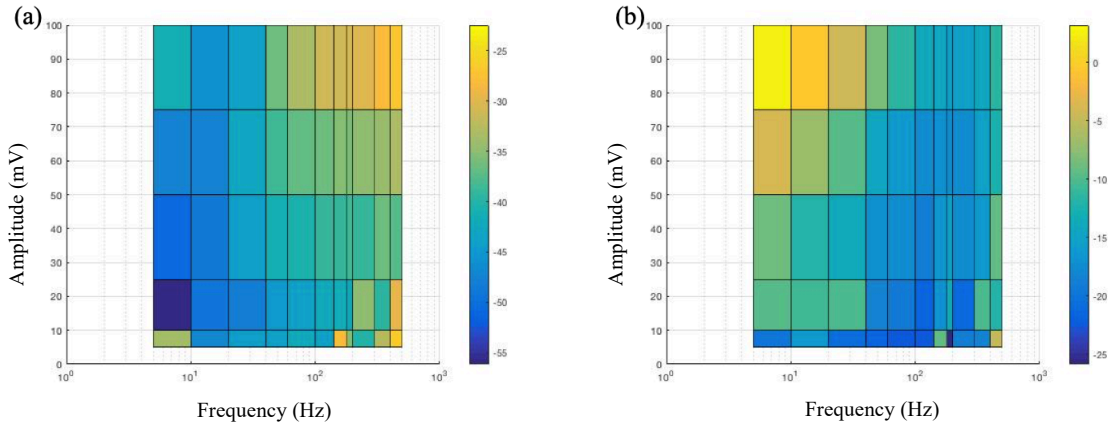

Figure 11: Frequency and amplitude tuning of the monovalent and bivalent FLAG epitope scaffold sensor. This is performed by taking the difference of all the signal output (current in microamps) for all of the frequency (5 – 500 Hz) and amplitude (10 – 100 mV) combinations in the absence and presence of saturating concentrations of anti-FLAG monoclonal antibody (30 nM) in phosphate buffered saline. (a) Frequency vs amplitude map of the monovalent FLAG epitope scaffold sensor. As illustrated by the figure, the maximum signal gain of the monovalent FLAG scaffold sensor is 55% and occurs at a frequency of 5 Hz and amplitude of 10 mV. (b) Comparatively, the maximum signal gain of the bivalent FLAG scaffold sensor occurs at a frequency of 120 Hz and amplitude of 10 mV, with a maximum binding induced signal gain of 25%.

2.4 Interpretations of results and conclusion

Detection limits are a function of both the gain of the sensor and the affinity of its receptor. Based on the results obtained (*Figures 8-11*), we conclude that the modifications utilized here with increased scaffold sensor flexibility and this bivalent epitope sensor architecture reduce signal gain enough to harm the limit of detection rather than improving it. However, only a few modifications to the E-DNA scaffold sensor architecture were investigated; future changes of the complementarity, length and placement of the redox reporter and integration of a second epitope may provide further improvements of the E-DNA scaffold sensor.

Chapter 3: Expansion to multiple disease biomarkers

3.1 Diagnosis of viral sexually transmitted infections using the E-DNA scaffold sensor

While sexually transmitted diseases are extremely prevalent, developed countries with access to routine healthcare and gold-standard STI testing methods (often government subsidized) typically see those infected receiving treatment, disease management, and a plan for long term follow up—all of which improve outcomes and quality of life while reducing disease transmission[51]. In rural or impoverished areas, in contrast, access to medical professionals and well-equipped diagnostic laboratories, and therefore treatment and long-term disease management, is often limited or even non-existent. Because of these factors, poor and geographically remote areas in developing countries are those with high prevalence, high mortality and increased risk of STI transmission. This high risk-low medical attention scenario is also mirrored by people displaced following natural disasters and refugees. Additionally, groups experiencing social stigma or living high-risk lifestyles, such as homosexuals, transgendered individuals, intravenous drug users, and sex workers, are seen to have a statistically significant higher prevalence of STIs, even in developed countries[6,19,43,52].

By increasing the efficiency of diagnosis, easily utilized point of care diagnostic devices that can be employed with minimal sample processing and no specialized training will reduce the number of patients in all demographics living with STIs and reduce transmission rates in these areas where routine health care is limited or interrupted. If a definitive diagnosis can be made before a patient is lost to follow up, treatment may eliminate a bacterial STI, or anti-viral therapies may prolong a patient's quality and length of life by decades[53]. We begin our expansion of the E-DNA scaffold sensing platform here, with

the aim of creating a point of care diagnostic tool that can detect multiple disease biomarkers in complex, minimally processed samples.

While incorporation of a full immunogenic antigen into our scaffold sensing architecture would allow for the detection of monoclonal and polyclonal antibodies for linear and conformational epitopes, our group has demonstrated that the signal gain of the scaffold sensor in response to the target antibody is directly proportionate to the size difference between the antigen/epitope displayed and antibody. Thus, utilization of short linear epitopes instead of full length or even truncated antigens provides an appreciably larger change in current as the result of a binding event[37]. Further, for this to be a viable diagnostic platform, considerations regarding sensor stability between fabrication and utilization at the point of care must be taken into account. Utilization of full-length or truncated proteins (but still folded) in our scaffold sensor presents several problems, most of which stem from the stability of a folded protein. Changes in temperature, electrolyte composition, and most importantly, time, affect a protein's ability to maintain its native, and therefore antigenic, structure[54]. The use of a linear, immunodominant epitope eliminates the problems that stem from maintaining a native state protein, and the E-DNA scaffold sensor employing linear epitopes for antibody detection have been shown to be stable over several weeks[17,31]. Our strategy for expanding the repertoire of diagnostic biomarkers in the E-DNA scaffold sensing platform is thus through identification of linear, immunodominant epitopes identified from the peer-reviewed literature.

3.2 Diagnosis of the human immunodeficiency virus using the E-DNA scaffold sensor

One of the most infamous, well studied, and high impact of the STIs is the human immunodeficiency virus (HIV), and the advanced and lethal state of HIV infection, acquired immunodeficiency syndrome (AIDS). As of the end of 2017, 36.9 million people are living with HIV, 1.8 million new people become infected with the virus each year, and in 2017 940,000 people died from HIV related causes globally[43]. However, with improvements in diagnostic speed and accuracy, patients have been able to make informed decisions to prevent the spread of HIV, with the rate of new HIV infections falling by 36% over the last 17 years[55].

Upon infection with HIV, the immune system undergoes an adaptive immune response against the pathogen: cell mediated immunity mediated by T lymphocytes, and humoral immunity mediated by antibodies produced by B cells[11]. Due to the structure and pathology of HIV, neutralizing antibodies from cell-mediated immunity are ineffective at killing the virus. Both these antibody types, however, are nevertheless of significant diagnostic importance. As the infection progresses the body produces an infection versus time dependent antibody profile against different HIV envelope proteins. Two of the most utilized diagnostic antibodies in clinical samples after infection with HIV are the early detection anti-p24 antibody, which shows up within a month after infection and disappears after six months, and the anti-gp41 antibody, which appears after four months and remains throughout the course of infection[56]. Based on these two antigen-antibody pairs, both lateral flow, point of care immunoassays and laboratory ELISAs have been developed and are widely employed in the diagnosis of HIV infection[43,55,57].

Although a literature search to identify linear epitopes in p24 identified no single immunodominant sequence, ample literature exists identifying a linear immunodominant epitope for the anti-gp41 antibody found in humans[17,43,58]. This linear epitope was identified via synthetic peptide epitope mapping, and further literature utilizing this identified antigenic peptide demonstrated excellent specificity and selectivity challenged with complex clinical samples[17,59]. The anti-gp41 antibody was found to recognize the amino acids CSGKLVC, and a human commercially available monoclonal antibody has been developed for purchase from Polymun Scientific for use as a positive control. Based on extensive literature showing this as a diagnostically significant peptide and the presence of a monoclonal antibody, this linear epitope was incorporated into E-DNA scaffold sensor platform, where we included an additional five amino acids taken from the original sequence of gp41 (LWGCSGKLVCTT) to minimize steric interactions.

The first experiment to validate the gp41 epitope sensor was to utilize a high affinity-custom designed ELISA to determine the binding potential and diagnostic predictive value of our PNA-epitope chimera when challenged with HIV positive and negative serum samples (see methods). Utilizing a 1:40 dilution of human serum and an anti-human horse radish peroxidase (HRP) conjugated secondary antibody, the scaffold sensor with and without the PNA was challenged using our ELISA protocol. As indicated by the results (*Figure 12*) the scaffold sensor with PNA was able to identify and differentiate between all of the positive samples and the negative controls. Background signal in the wells without the PNA containing epitope, due to non-specific adsorption of antibodies present in human serum, was relatively low and did not provide any false positives. Based on these ELISA results, we

anticipated that our E-DNA scaffold sensor would similarly achieve > 95% positive and negative predictive value as required by WHO rapid test guidelines[43,53,60].

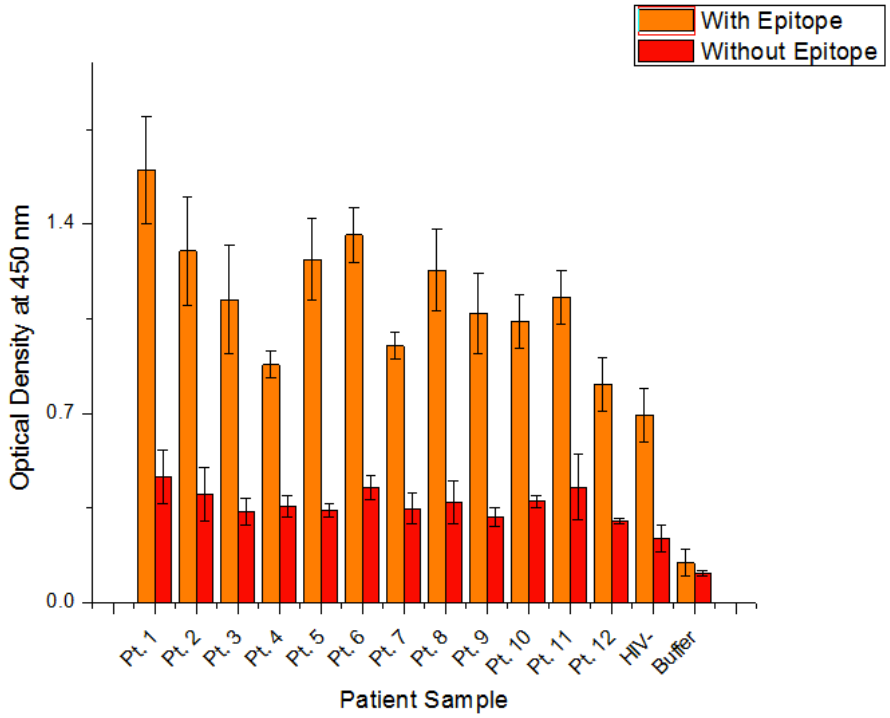

Figure 12: Custom PNA scaffold ELISA of the gp41 immunodominant epitope against HIV seropositive and seronegative patient samples. In red is the background signal due to nonspecific adsorption in the absence of the PNA and linear epitope, and in orange with have the signal with the PNA and anti-gp41 linear immunodominant epitope due to antibody-epitope interactions. As demonstrated by the figure above, this linear epitope demonstrates positive and negative predictive value for HIV positive and negative serum sample by ELISA. Data points are comprised of an average and the error bars are the standard error (n=3).

With the positive results from ELISA indicating diagnostic success for the gp41 PNA, next step was to evaluate its success on the electrode surface. More importantly, we want to demonstrate that it is the presence of the anti-gp41 diagnostic antibody, and not the other antibodies or components of complex clinical samples that gives rise to an observable signal. Anticipating less sensitivity than an ELISA, the gp41 sensor was challenged with 1:10 dilutions of either known HIV positive human serum (patient 1 in ELISA) or known HIV

negative serum in buffer (3x phosphate buffered saline, 0.05% Tween-20, 1% bovine serum albumin). Next, the antibodies in HIV positive serum were removed using a protein G spin trap, and the sensor was challenged with the antibody depleted serum. Finally, the sensor was challenged with 30 nM of the commercially available anti-gp41 antibody that was spiked into HIV negative serum. For each of these conditions, the electrodes in triplicate were allowed to equilibrate for thirty minutes before interrogation via square wave voltammetry at a frequency pulse of 100 Hz and amplitude of 25 mV[17]. The FLAG epitope scaffold sensor was used as a negative control.

The results (*Figure 14*) indicate that the gp41 scaffold sensor has a signal gain of ~38% when challenged with dilute positive serum from patient sample 1. Comparatively, when challenged with dilute known negative serum and antibody removed positive serum, the gp41 scaffold sensor only exhibits of signal change of ~8%. Lastly, when the sensor is challenged with the dilute HIV negative serum spiked with anti-gp41 monoclonal antibody, we again see an appreciable, diagnostically significant signal of ~25%. The FLAG sensor throughout, and the signal of the gp41 sensor in response to negative and antibody depleted serum, was consistently under 10%. Based on the complexity of clinical samples, even when dilute, it is within the realm of expectation that these relatively low changes in signal are due to the nonspecific adsorption that occurs in complex samples.

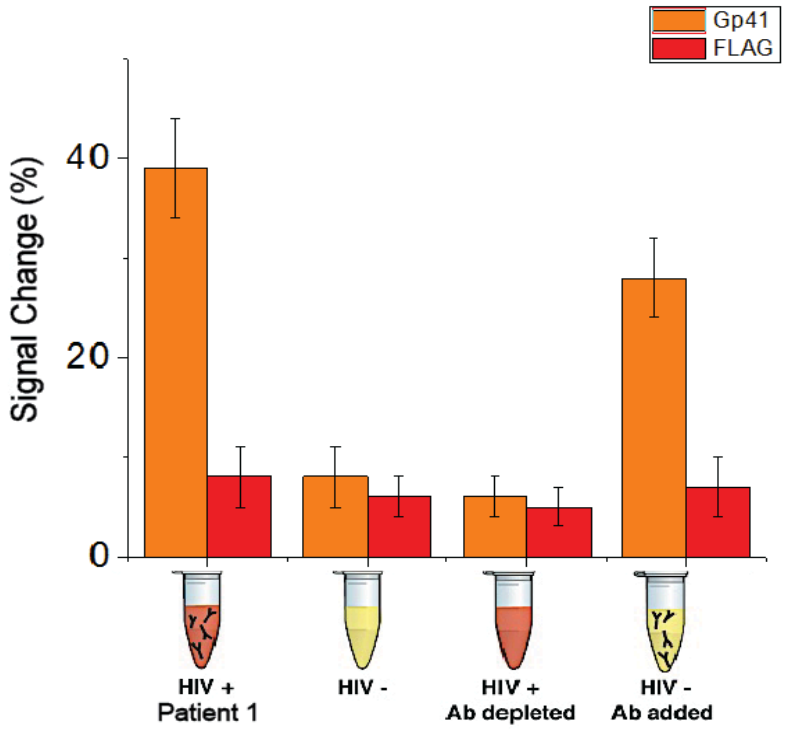

Figure 13: The gp41 E-DNA scaffold sensor selectively binds antibodies specific to HIV infection. This figure illustrates the electrochemical response of the gp41 scaffold sensor to positive serum, negative serum, antibody depleted positive serum, and negative serum spiked with commercially available human anti-gp41 antibodies. As demonstrated by the figure, the gp41 scaffold sensor has a gain of 38% in positive serum yet does not respond to HIV negative human serum (8%) or HIV positive serum with the antibodies removed (6%). When challenged with anti-gp41 monoclonal antibodies in negative serum, the sensor again demonstrates a diagnostically significant signal of 24%. In all scenarios, the FLAG scaffold sensor does not display a signal gain of more than 10%, which is within the realm of signal gain due to nonspecific adsorption in complex clinical samples. All of the serum samples evaluated above were diluted 1:10 in buffer. Data points are comprised of an average and the error bars are the standard error (n=3).

To further validate our sensing platform and its utilization for point of care diagnostics, equilibration time and sensor binding kinetics in a complex clinical sample was studied. To accomplish this, the gp41 and FLAG sensors were challenged with 1:10 diluted negative human serum in 3x phosphate buffered saline. This solution was then spiked with saturating concentrations (30 nM) of human anti-gp41 monoclonal antibody. The electrodes were scanned using square wave voltammetry at a frequency of 100 Hz and amplitude of 25mV. Plotting signal change as a function of time, we see rapid equilibration of the gp41

sensor in the presence of saturating concentrations of target antibody (*Figure 14)*. Within the 15-minute point of care diagnostic window, we see that while the control FLAG sensor exhibits a signal change of ~5%, the gp41 signal changes by ~25%. These results demonstrate that the equilibration of the gp41 sensor is rapid enough to provide actionable diagnostic information within the short time frame consistent with point of care applications.

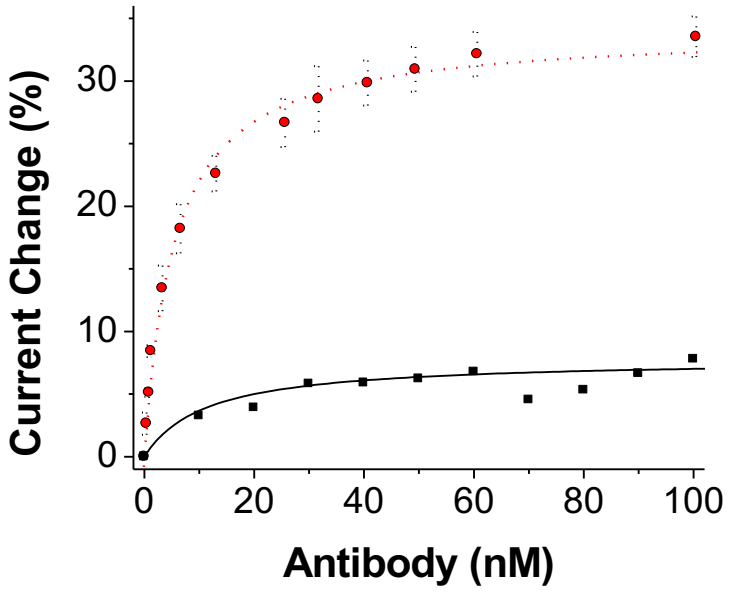

Figure 14: Rapid equilibration of the gp41 E-DNA scaffold sensor. Kinetic study of the gp41 and FLAG sensor in negative serum with saturating concentrations of the human anti-gp41 monoclonal antibody (30 nM). Within 15 minutes the gp41 scaffold sensor (red) exhibits a signal gain of 18%, whereas the signal gain by the control FLAG scaffold sensor (black) is less than 5%. Data points are comprised of an average and the error bars are the standard error (n=3).

As demonstrated in the prior two figures, the gp41 scaffold sensor selectively, specifically, and rapidly binds to anti-gp41 antibodies present only in HIV positive serum, for at least one sample. To further expand this claim, under identical serum dilution and electrochemical conditions described for the previous experiment, we challenged the gp41 scaffold sensor with the remaining patient serum samples used in the ELISA after allowing electrodes to equilibrate for 20 minutes. As seen in *Figure 15*, all but two of known positive

HIV serum samples did not provide a diagnostically significant electrochemical signal (e.g., did not have a signal at least one standard deviation higher than the negative control). For the electrodes that did produce a diagnostically significant signal, the signal change varied between ~16 and 28%. Overall, 84% of patient serum samples that were identified seropositive for anti-HIV antibodies, both by the supplier and by our ELISA, elicited a diagnostically actionable electrochemical signal. We believe this false-negative response to be due to a concentration of anti-gp41antibody that is below the limit of detection for our sensors. Because ELISA is orders of magnitude more sensitive than our electrochemical tests, it is reasonable to speculate that ELISA would be able to detect diagnostically significant concentrations of antibodies where our sensor would not.

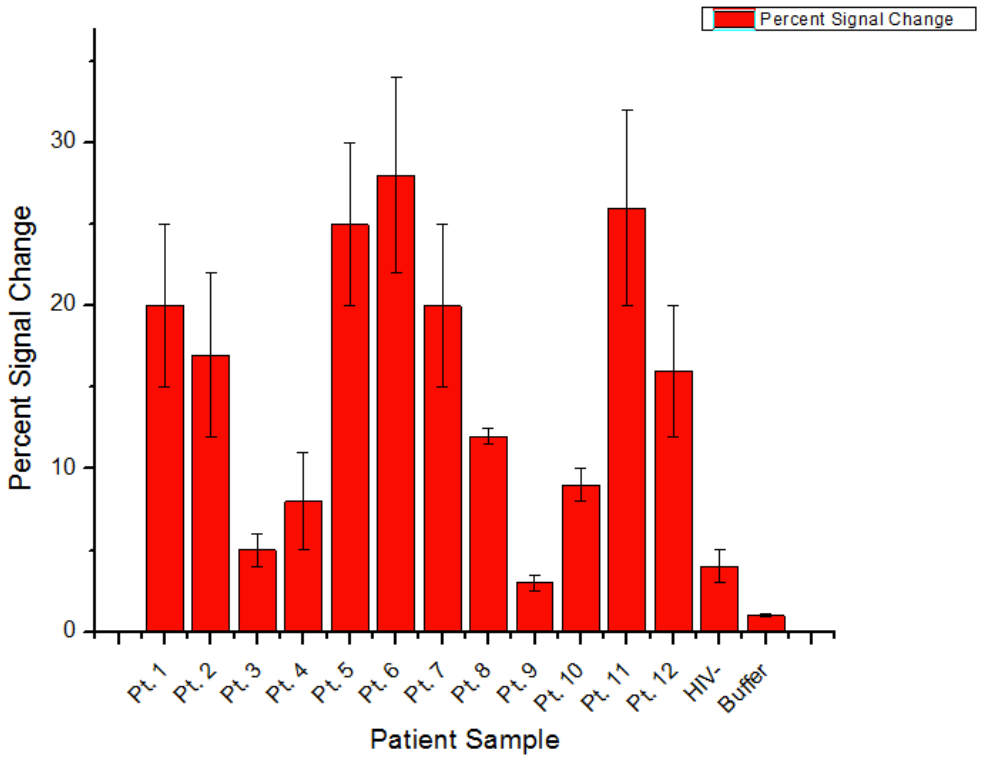

Figure 15: Electrochemical response of the gp41 E-DNA scaffold sensors to various known positive and negative patient serum samples. Out of twelve known HIV positive serum samples, the gp41 E-DNA scaffold sensor demonstrated significant signal gain to positively identify ten samples, with two serum samples demonstrating low signal gain that is within one standard deviation of the negative control, HIV negative serum. Data points are comprised of an average and the error bars are the standard error (n=3). The high error bars here are likely due to sensor-to-sensor variability, which is the result of hand fabrication of electrodes.

3.3 Diagnosis of hepatitis C infection using the E-DNA scaffold sensor

Infection by the hepatitis C virus (HCV) produces liver disease with two modalities: acute, which results in mild illness lasting several weeks, or chronic, which is a lifelong illness. While both modalities are serious, chronic HCV typically results in permanent liver damage, which manifests as either chronic cirrhosis or hepatic cancer. Per WHO statistics, chronic HCV affects an estimated 71 million people globally, with approximately 400,000 deaths and 1.75 million new infections annually[55]. In recent years, antiviral therapeutics have been developed which can cure approximately 95% of patients living with the chronic

disease. Limited access to diagnostic assays and medical treatment still makes HCV extremely prevalent. Like HIV, high-risk demographics, including intravenous drug users and commercial sex workers, have higher infection and transmission rates. Additional modes of transmission include inadequate sterilization of medical supplies and tainted blood transfusions[61].

Most people experiencing acute HCV infection are asymptomatic, and even people with chronic infections can remain asymptomatic for decades[62]. Surprisingly, between 15 and 45% of people who contract the disease clear the virus without medical intervention. Because of spontaneous clearance of the virus due to a strong immune response, which can result in a lifetime presence of anti-HCV antibodies, people exhibiting symptoms of HCV are often given two tests[43]. The first diagnostic test is ELISA against anti-HCV antibodies. Because there is not clear immunogenic prevalence for one protein of HCV, first, second and third generation ELISAs have all employed a variety of recombinant epitopes from multiple antigens, or multiple full-length antigens[62]. If the anti-HCV antibody ELISA is positive, a secondary test is performed which uses a PCR reaction to test for the presence of hepatitis C viral RNA. In the case of a positive ELISA and a negative HCV PRC reaction, a RIBA is performed which tests for the presence of antigen specific anti-HCV antibodies. This test is typically employed to determine if the patient has a resolved HCV infection of a biological false positive ELISA[63]. Diagnosis of HCV using ELISA, PCR and RIBA is an intensive, time consuming processes that requires trained technicians and expensive equipment to perform[62].

Only within the last two years has the first point of care diagnostic test been prequalified for use by the WHO to aid in the diagnosis of HCV in low income and developing countries[64]. This device is a LIA that utilizes three of HCV's ten proteins[62] for

diagnosis in complex samples in 20 minutes. When compared to the commercially available RIBA, the new point of care LIA only demonstrated 78.8% sensitivity. In contrast, however, it achieved 100% specificity when challenged with clinical samples positive for hepatitis B and other potentially cross-reactive diseases[20]. While being the first of its kind, the low sensitivity and high number of target antigens used in this HCV diagnostic LIA necessitates secondary testing and larger blood volumes with diagnostic times outside the point of care window[3]. While this test meets the WHO criteria ASSURED, improved sensitivity for the point of care detection of anti-HCV antibodies is necessary to increase diagnostic efficacy and assist in the eradication HCV.

One of the HCV proteins that has consistently been employed in multiple generations of ELISA and RIBA to diagnose HCV is the core protein[62]. Epitope mapping of this protein using synthetic peptides challenged with 96 human serum samples (50 positives and 46 negatives by full-length antigen ELISA) indicates two overlapping linear immunodominant sequences. The first consists of amino acids 1-18 and exhibits 80% clinical specificity and the second spans from amino acids 11-28 and exhibits 82% specificity, where both demonstrated 100% clinical sensitivity by ELISA. When these two synthetic peptides were employed in tandem (as separate peptides) and tested against the same set of 96 serum samples, they yielded 92% specificity while maintaining 100% selectivity[65]. Further study over the next decade by multiple independent research groups consistently demonstrated the same findings[7,66–68]. Based on these results found in the literature, the two overlapping linear epitopes, consisting of amino acids 1-28 of the HCV core protein (MSTNPKPQRKTKRNTNRRPQDVKFPG), were incorporated into our E-DNA scaffold sensor architecture.

Our first experiment to determine the ability of our HCV PNA to detect anti-HCV antibodies indicative of infection and differentiate them from normal human serum, was the ELISA. Using the protocol described in the methods, the HCV PNA was challenged with 1:80 dilutions of known positive and negative serum samples using FLAG as an additional negative control. As seen in *Figure 16*, when compared the absorbance to HCV negative serum, seven of the ten known seropositive samples were highly reactive to the HCV PNA, whereas one was moderately reactive, and two samples were nonreactive. However, this result is within the realm of acceptability, namely because previous studies that tested the diagnostic potential of this epitope used significantly more samples, and the specificity of this epitope has not been shown to be 100%.

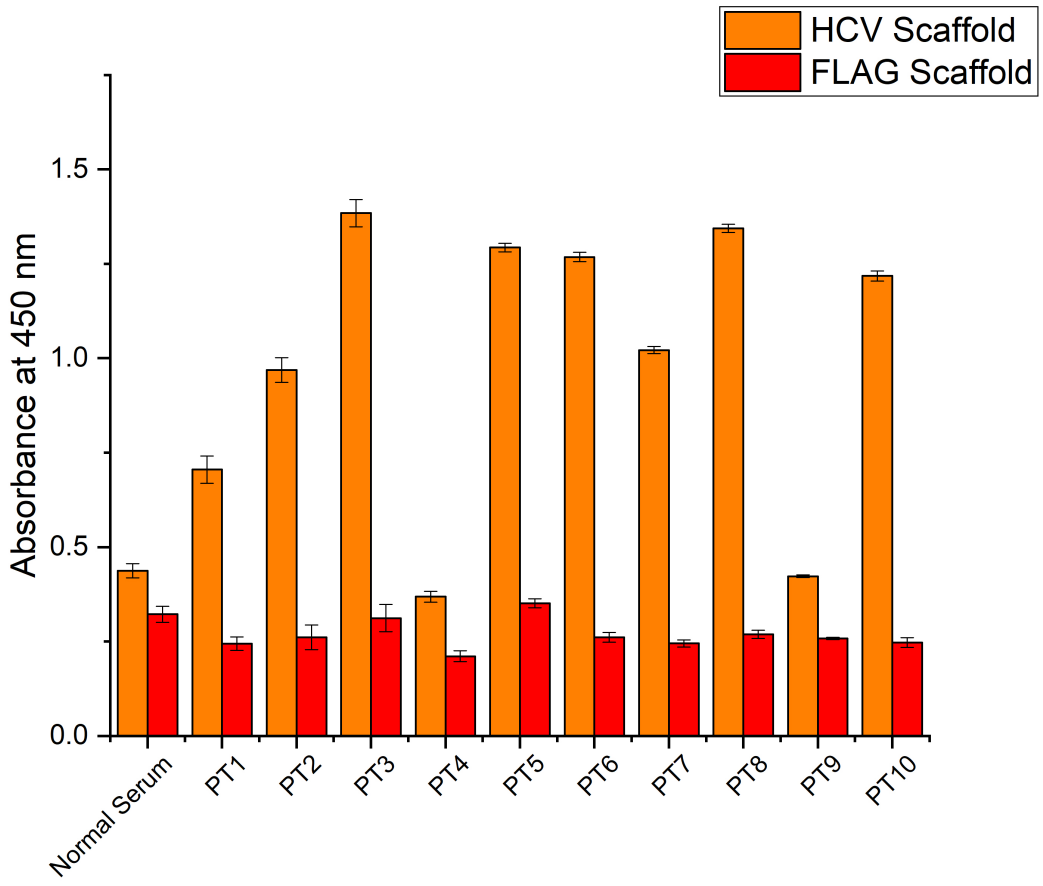

Figure 16: Custom PNA scaffold ELISA of the HCV PNA against HCV seropositive and seronegative patient samples. As illustrated by the figure, eight out of ten serum samples were identified as positive using our linear immunodominant epitope, with the remaining two serum samples providing a signal that was less than, or within one standard deviation of the negative control, normal serum. The FLAG PNA was used as a control, demonstrating no cross-reactivity between the FLAG epitope and the HCV seropositive samples. Data points are comprised of a three well average and the error bars are the standard error.

Based on the reactivity of the sensor by our custom ELISA, the HCV PNA was incorporated into our E-DNA scaffold sensor and challenged with the same clinical samples used in above ELISA. Using square wave voltammetry at a frequency of 60 Hz and amplitude of 25 mV, the E-DNA scaffold sensor containing the HCV PNA failed to demonstrate a diagnostically significant signal gain in response to anti-HCV antibodies from HCV positive patients two, three and eight when compared with the control FLAG PNA (1:10 diluted serum in 3x phosphate buffered saline) (*Figure 17*). Even though these were the

most reactive patient samples by ELISA, and even with repetitions of this experiment where nonspecific adsorption was blocked on the electrode surface (using 3x PBS, 0.05% tween-20, 1 mg/mL fibrinogen), the sensors failed to respond appreciably to HCV positive serum.

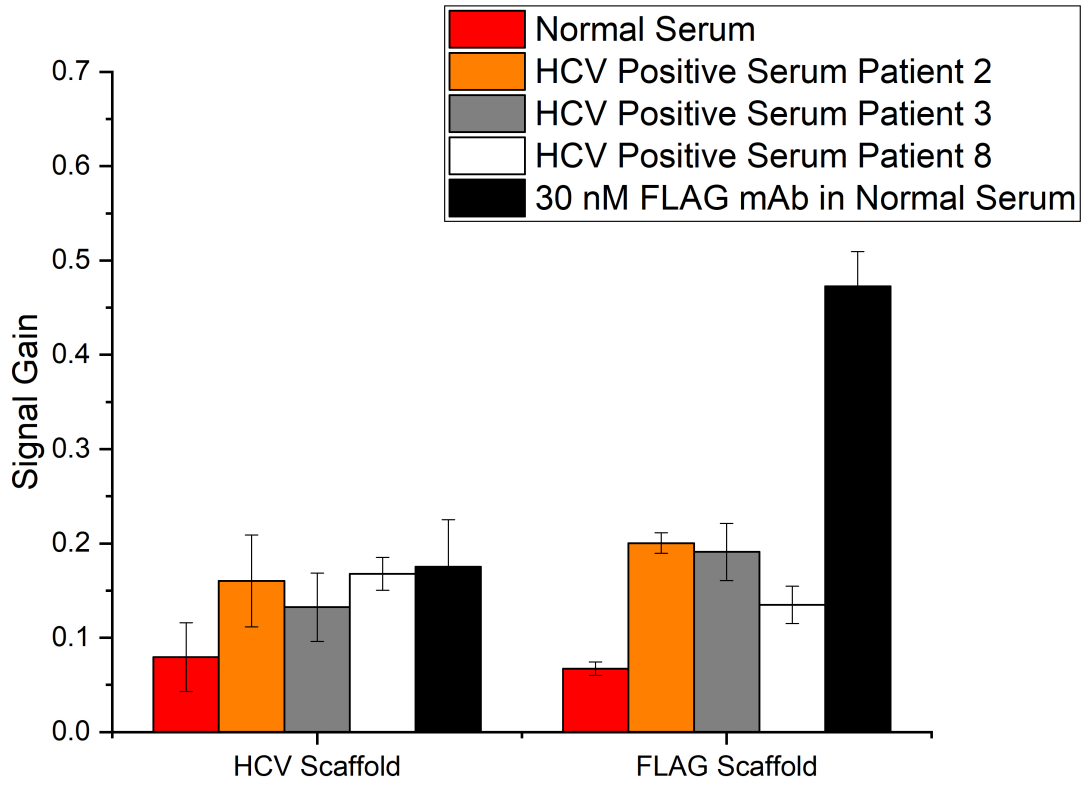

Figure 17: Electrochemical response of the HCV scaffold sensor over an hour to 1:10 diluted normal serum and HCV seropositive patient samples. Based on the results presented in the figure, there was no statistically significant signal gain by the HCV scaffold sensor (right) in response to known positive serum samples two (orange), three (grey), or eight (white) when compared to normal serum (red) and to the response by the control FLAG scaffold sensor (left). Sensor batch assembly and functionality success was verified by challenging the HCV and FLAG scaffold sensors in 1:10 diluted normal serum spiked with saturating concentrations (30 nM) of anti-FLAG monoclonal antibody (black). As seen, the control FLAG scaffold sensor underwent a signal gain of 48% (net 30%) over the course of an hour in response to anti-FLAG monoclonal antibody, indicating the scaffold sensors were successfully built on the surface. Data points are comprised of a three-electrode average and the error bars are the standard error.

Because the ELISA is orders of magnitude more sensitive than our E-DNA scaffold sensor it is possible that the concentration of anti-HCV antibodies present in these HCV

patient serum samples is below the limit of detection of the E-DNA scaffold sensor. While this process does require significant processing of clinical samples, 1 mL of serum from patient samples two, three, and five underwent antibody removal using a protein G spin trap and were subsequently concentrated using a 15 kDa centrifugal filter unit. The HCV and FLAG scaffold sensors were than challenged with these concentrated antibodies at a final concentration of ten times the concentration of 100% serum (henceforth referred to as 10x concentrated antibodies) in 3x phosphate buffered saline under identical square wave voltammetry experimental conditions. As seen in *Figure 18,* when compared to the FLAG control, the HCV scaffold sensor does not exhibit any specific, binding-induced signal change in response anti-HCV antibodies, even when concentrated. Even if the HCV sensor were able to detect removed, concentrated anti-HCV antibodies, the significant post collection sample processing required would eliminate the epitope used in this HCV scaffold sensor for use as a point of care diagnostic test.

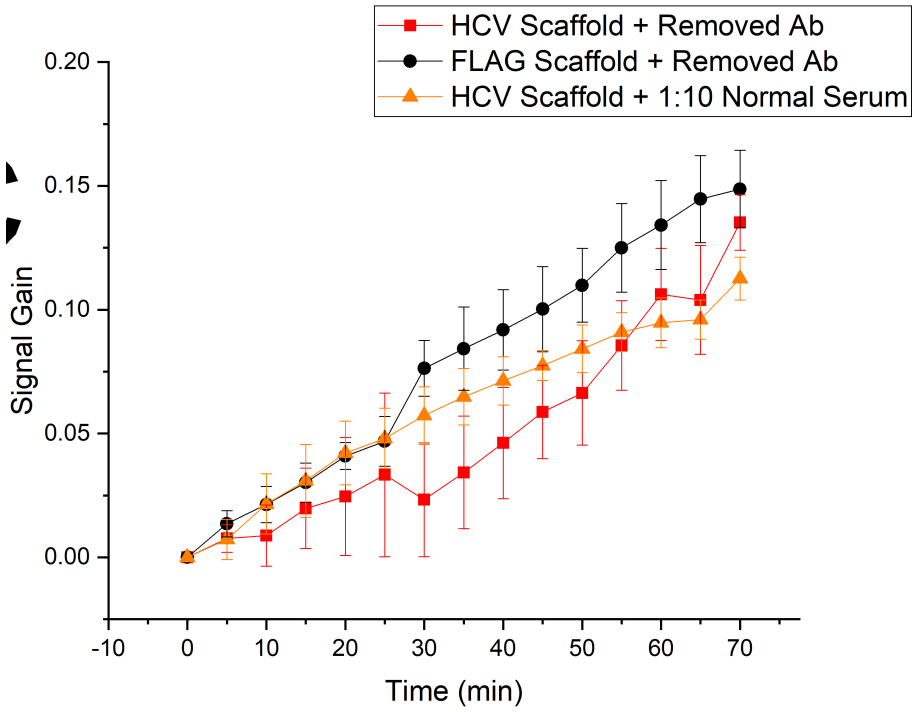

Figure 18: HCV scaffold sensor challenged with antibodies removed and concentrated from the four most reactive HCV seropositive patients by ELISA (patients 2,3,5 and 8). Antibodies were removed using a protein G spin trap and concentrated using size exclusion protein concentrators. Removed and concentrated antibodies from the HCV serum were spiked into 3x phosphate buffer to a final concentration of ten times their concentration in 100% serum. As demonstrated by the figure, there is no statistically significant signal gain by the HCV scaffold sensor (red) in the presence of removed and concentrated antibodies buffer when compared to the response of the FLAG scaffold sensor (black) and the HCV scaffold sensor in 1:10 diluted normal serum in 3x phosphate buffer (orange). All signal gain can be attributed to drift, as evidenced by nearly identical signal gain by the FLAG scaffold sensor and HCV scaffold sensor in 1:10 diluted normal serum. Data points are comprised of an average and the error bars are the standard error (n=3).

3.4 Diagnosis of the herpes simplex type 2 virus using the E-DNA scaffold sensor

Herpes simplex virus (HSV) is an increasingly common, highly contagious disease affecting approximately half a billion people between the ages of 15-49[43,52]. Two genetically distinct variations of the HSV exist, types 1 (HSV-1) and two (HSV-2). A common misconception is that HSV-1 is solely responsible for oral herpes and HSV-2 is solely responsible for genital herpes, when in actuality both variations of the virus can infect the same anatomical area[69]. However, HSV-2 infections have a much higher recurrence rate (~5x

greater), and thus symptoms leading to repeated clinical visits which prompt diagnostic testing usually are the result of the HSV-2 variant[6]. Unfortunately, patients presenting with symptoms are often the only ones with the disease diagnosed by a clinician, with diagnosis rates between 13 and 37%, despite the high prevalence of the disease. Simply put, patients not experiencing HSV symptoms are not typically tested for the disease and can go undiagnosed for years. However, patients not presenting with HSV symptoms who are known positives for other sexually transmitted infections typically have a higher testing frequency and therefore higher diagnosis rate[70,71].

The primary antigen used to detect anti-HSV-2 antibodies and to differentiate between HSV-2 infection and infection with the closely related HSV-1 is a highly immunogenic external glycoprotein G2 (gG2)[72,73]. Current diagnosis of asymptomatic HSV-2 is performed in two phases: the first, which provides a preliminary diagnosis and immediate actionable information, is a LIA against gG2 specific antibodies[74], the second, which confirms the diagnosis, is a gG2 specific ELISA[75]. Epitope mapping using overlapping synthetic peptides of gG2 identified a 19 amino acid sequence with excellent clinical sensitivity and specificity when used in ELISAs[74,76–78]. Here we incorporated this immunodominant epitope (PEEFEGAGDGEPPEDDDS) into our scaffold sensor platform to electrochemically detect anti-HSV-2 antibodies in serum.

The first test of our sensor was to determine if the sensor can differentiate between HSV-2 positive and negative serum using our custom ELISA. To test this, we challenged the sensor with 12 known seropositive and one seronegative clinical HSV-2 samples. While the gG2 linear epitope was able to distinguish between known positive and negative clinical samples at a 1:10 dilution (*Figure 19*), there are two concerning aspects of this data: 1) the

signal of the ELISA is extremely low in known positive serum samples at a relatively high concentration of serum and 2) the most reactive of the positive patient samples exhibit a signal gain of approximately twice that of the negative control.

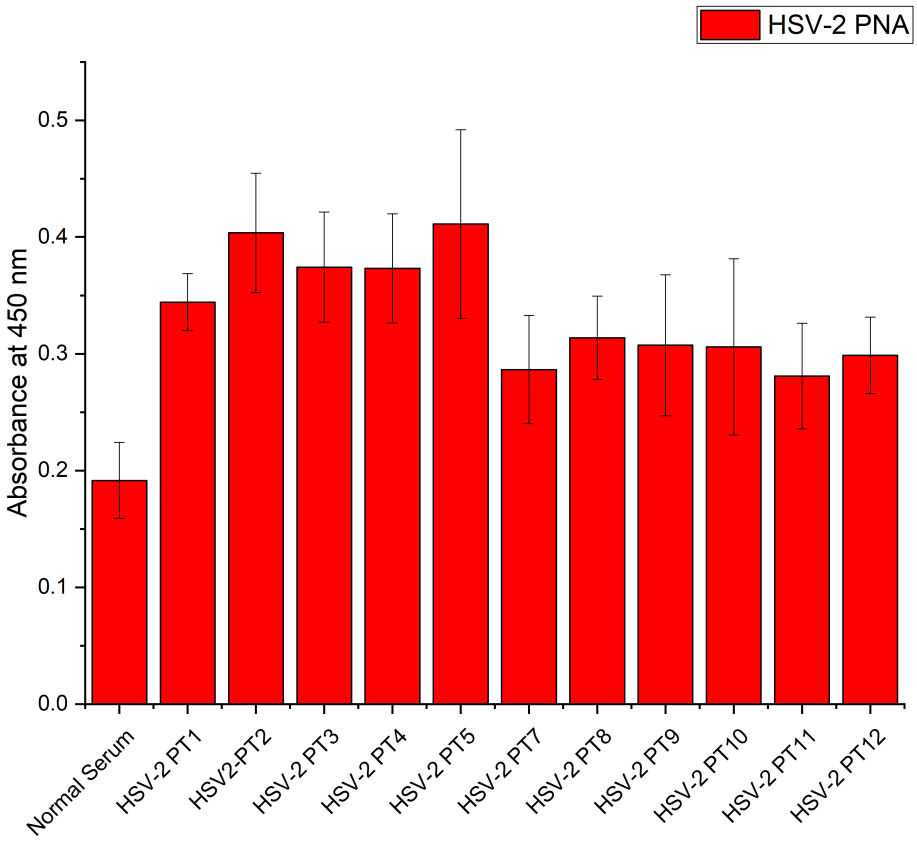

Figure 19: Custom PNA scaffold ELISA of the HSV-2 immunodominant epitope against HSV-2 seropositive and seronegative patient samples. As illustrated by the figure, all the serum samples were identified as positive using our linear immunodominant epitope when compared with a negative control, HIV positive patient sample 6. It is important to note that while all twelve of the known positive serum samples here are definitely identified as positive using the HSV-2 PNA, the absorbance values are significantly lower than those usually seen by ELISA, with repetitions of this experiment yielded similar results. Data points are comprised of a three well average and the error bars are the standard error.

Nonetheless, based on the above result the gG2 linear epitope was incorporated into the scaffold sensor architecture on the electrode surface and challenged with 1:10 dilutions of known positive and negative serum. Initial results, which are not included here, showed

substantial variability in signal when the HSV-2 scaffold sensor was challenged with the same 1:10 diluted pooled sample of negative serum (6 to 35% signal change). Based on the results from the ELISA experiment, the scaffold sensor was challenged with the two most reactive HSV-2 patient samples, two and five. To minimize the variability of the sensors in response to negative, and potentially positive serum, the electrodes were "pre-blocked" using 1:10 negative serum, before being challenged with 1:10 HSV-2 positive serum in 3x phosphate buffered saline. The FLAG sensor was run in parallel, in identical experimental conditions to serve as a negative control in the presence of HSV-2 negative and positive serum. Following a one hour of equilibration of the electrodes in positive serum, the sample cell was spiked with saturating concentrations of anti-FLAG monoclonal antibody, wherein the FLAG sensor served as an internal positive control. These results, found in *Figure 20*, demonstrate no significant signal gain, and therefore differentiation, between positive and negative serum by the HSV-2 scaffold sensor. This negative result is further validated by a nearly identical signal change by the negative control FLAG sensor in both systems. Upon addition of anti-flag monoclonal antibody, the FLAG sensor exhibited a significant signal change (~30%) within 15 minutes of addition of anti-FLAG monoclonal antibody (mAb), indicating no error in sensor fabrication. Further experimentation, where the gG2 epitope was challenged with removed and concentrated antibodies from the most reactive by ELISA HSV-2 serum samples, demonstrated no specific binding induced signal gain. When challenged with 10x concentrated antibodies in 3x phosphate buffered saline, the signal gain by the HSV-2 sensor was mirrored by the FLAG sensor, which was used as control.

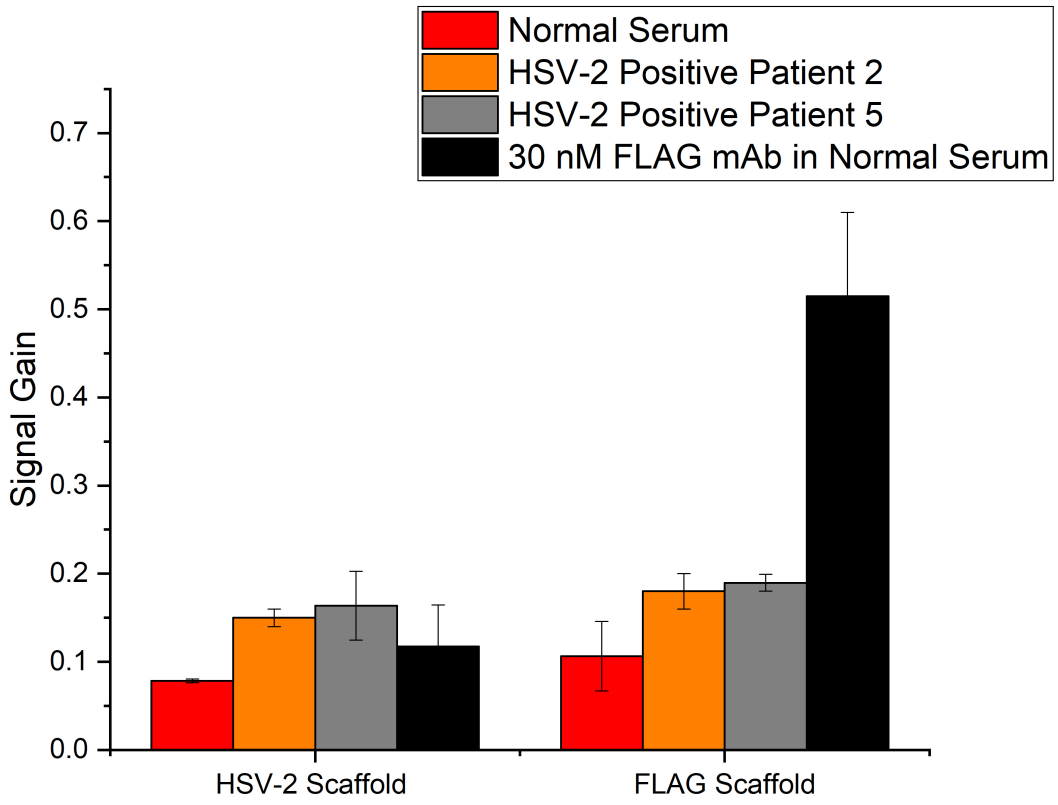

Figure 20: Electrochemical response of the HSV-2 scaffold sensor over an hour to 1:10 diluted normal serum and the most reactive by ELISA HSV-2 seropositive patient samples. Based on the results presented in the figure, there was no statistically significant signal gain by the HSV-2 scaffold sensor (right) in response to known positive serum samples two (orange) or five (grey) when compared to normal serum (red) and to the response of the control FLAG scaffold sensor (left). Sensor batch assembly and functionality success was verified by challenging the HSV-2 and FLAG scaffold sensors in 1:10 diluted normal serum spiked with saturating concentrations (30 nM) of anti-FLAG monoclonal antibody (black). As seen, the control FLAG scaffold sensor underwent a signal gain of 53% (net 40%) over the course of an hour in response to anti-FLAG monoclonal antibody, indicating the scaffold sensors were successfully built on the surface. Data points are comprised of a three-electrode average and the error bars are the standard error.

Before declaring the project a failure, additional exploration of the literature produced work by Liljeqvist and collaborators[79], who demonstrated that the antibody-binding site for gG2 epitope actually begins five amino acids residues towards the amino-terminus of the full length protein and continued into the first three amino acids of our HSV-2 PNA epitope (HRGGPEE). This finding was corroborated by the results of a collaborator, Dr. Michael Paull, who screened our collection of HSV-2 positive serum samples against random surface

displayed peptide library[80]. Upon antibody binding to one of the surface displayed peptides, the antibody and the bacteria displaying the peptide were removed using protein A/G conjugated magnetic beads, which yielded a patient specific antigenic peptide library. Immunodominant motifs identified using this method were then compared between HSV-2 samples, and then compared to the linear amino acid sequence of gG2. Surprisingly, all twelve HSV-2 positive patient samples displayed immunogenicity to the sequence (GGPEEFEGAGD). When compared to the originally utilized HSV-2 epitope (PEEFEGAGDGEPPEDDDS), it becomes clear that if the antibody is binding to our HSV-2 epitope, greater than half of the epitope is not present. Additionally, if the antibody is binding to our PNA, it is binding where it attaches to the DNA/PNA duplex and a long, unbound tail of amino acids is free to interact with the components of the serum, which could further diminish peptide-antibody binding and increase non-specific binding events and steric effects. As a result, a new linear epitope (HRGGPEEFEGAGD) incorporating both additional findings was employed for our scaffold sensor platform.

Despite our expectations, fine-tuning of the immunodominant gG2 linear epitope to include the reported antibody binding site did not improve our sensors performance. Initial testing by our custom ELISA employing a 1:80 dilution of brand-new patient serum samples, yielded high background from the two control sensors employed (FLAG and gp41) with little to no statistically significant signal change due to the presence of the anti-gG2 antibody in six positive patient serum samples. Furthermore, the negative control (normal serum) demonstrated a similarly high signal, which indicates that only three of the six newly acquired patient serum samples is can be diagnosed as positive using this epitope by ELISA (*Figure 21*). Despite the less than optimal results from the ELISA, the new HSV-2 scaffold

sensor was challenged electrochemically (frequency 60 Hz and amplitude 25 mV) with the most reactive by ELISA HSV-2 positive serum samples (patients four and two diluted 1:10 in 3x phosphate buffered saline). The results, presented in *Figure 22*, demonstrated no statistically significant signal gain when compared to the response from 1:10 diluted normal serum in 3x phosphate buffered saline, and the control gp41 scaffold sensor in identical experimental conditions. As a last-ditch effort, three of the most reactive of the new HSV-2 serum samples were pooled, had the antibodies removed via protein G spin trap, and then concentrated. When the new HSV-2 scaffold sensor was challenged electrochemically with 3x phosphate buffered saline containing 10x concentrated antibodies, with the gp41 and FLAG sensors in the same solution as controls, the only signal gain observed was due to sensor drift and/or the nonspecific adsorption of antibodies, as the signal gain of the HSV-2 scaffold sensor was mirrored by both controls (*Figure 23*).

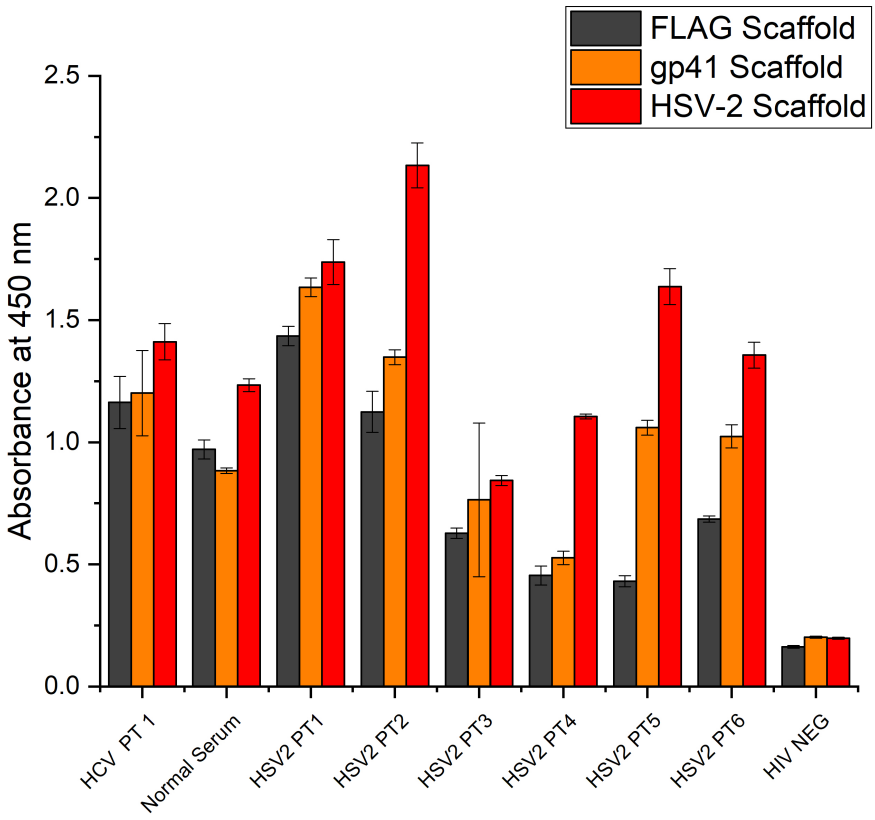

Figure 21: Custom PNA scaffold ELISA of the redesigned HSV-2 immunodominant epitope against newly purchased HSV-2 seropositive and seronegative patient samples. As illustrated by the figure, three out of six serum samples were identified as positive using this linear immunodominant epitope, with the remaining three serum samples providing a signal that was less than, or within one standard deviation of the negative controls, either HIV negative serum pool or normal serum. HCV seropositive patient sample 1 was included in this experiment in the hopes of identifying a dual disease state patient sample. The signal of this sample is so close to the normal serum sample, determination of dual infection modalities is inconclusive from this data. Here, the FLAG (black) and gp41 (orange) PNA were used as a control, demonstrating abnormally high signal in response to all serum (save HIV negative). Subsequent optimization and blocking conditions, washing, and optimization of secondary antibody concentration still showed high background signal from FLAG and gp41 PNA controls. Data points are comprised of a three well average and the error bars represent the standard error.

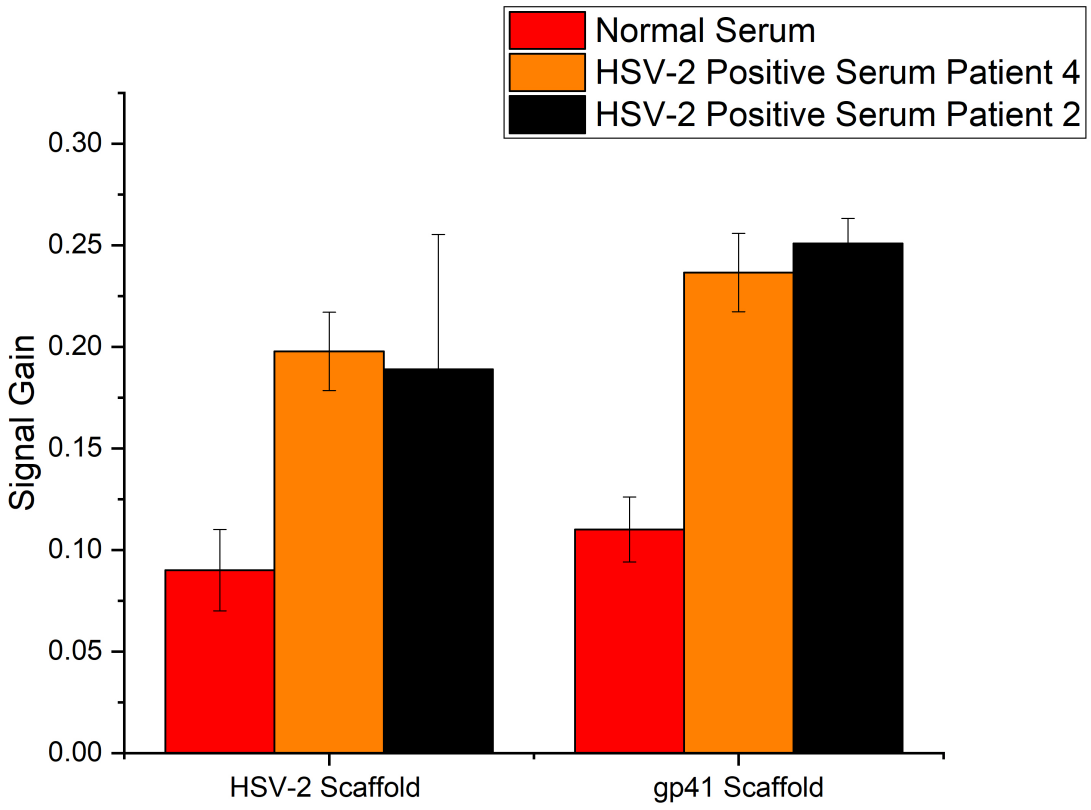

Figure 22: Electrochemical response of the redesigned HSV-2 scaffold sensor over an hour to 1:10 diluted normal serum and the most reactive by ELISA HSV-2 seropositive patient samples. Based on the results presented in the figure, there was no diagnostically significant signal gain by the HSV-2 scaffold sensor (left) in response to known positive serum samples four (orange) or two (black) when compared normal serum (red) and the control gp41 scaffold sensor (right). Data points are comprised of a three-electrode average and the error bars are the standard error.

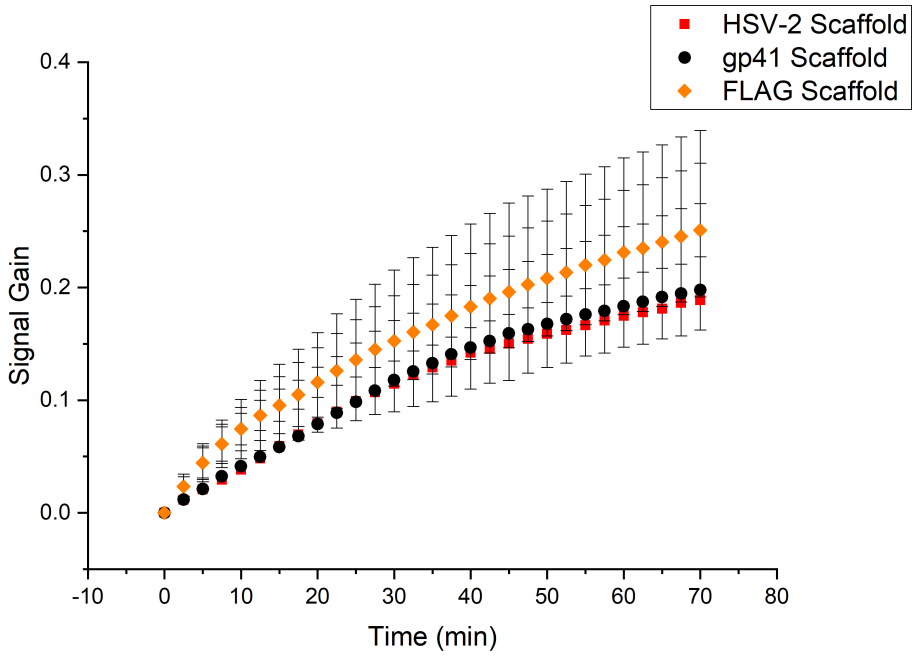

Figure 23: Redesigned HSV-2 scaffold sensor challenged with antibodies removed and concentrated from the three most reactive HSV-2 seropositive patients by ELISA (patients 1,2 and 5). Antibodies were removed using a protein G spin trap and concentrated using size exclusion protein concentrators. Removed and concentrated antibodies from the HSV-2 serum were spiked into 3x phosphate buffer to a final concentration of ten times their concentration in 100% serum. As demonstrated by the figure, there is no statistically significant signal gain by the HSV-2 scaffold sensor (red) in the presence of removed and concentrated antibodies in buffer, as evidenced by nearly identical signal gain by the FLAG (orange) and gp41 (black) scaffold sensors, which was used as a control. Data points are comprised of an average and the error bars are the standard error (n=3).

3.5 Discussion about the expansion of multiple biomarkers and general trends observed

Overall, successful expansion of our E-DNA scaffold sensing platform to include linear epitopes diagnostically relevant for additional diseases has remained elusive. Save for the initial success with the anti-gp41 linear epitope[17,40], the results above demonstrate the difficulty of integrating linear epitopes for HCV and HSV-2 into our platform *(Figures 16-23).* The most pressing problem is the result of a limited understanding of our E-DNA scaffold sensor chemistry: a diagnostic synthetic peptide from literature that demonstrates a high binding affinity by commercial and custom scaffold sensor ELISA subsequently fails

when challenged with positive human serum on the electrode surface. Through this work, a set of experiments has been identified to quickly eliminate a linear epitope as unsuitable for the E-DNA scaffold sensing platform. A plethora of other linear epitopes, for multiple diseases, including but not limited to STIs, exist and can be successfully integrated into our E-DNA scaffold sensor for diagnosis.

Chapter 4: Conclusions

In response to the need for quantitative point of care serology we have developed a reagentless, electrochemical platform for the measurement of specific antibodies in complex clinical samples[17,31,81]. These consist of a short, relatively rigid nucleic acid duplex scaffold anchored at one end to a gold electrode via a flexible linker and modified on their other end with a redox reporter and an antibody-binding epitope. In the absence of the target antibody, the flexibility of the linker allows the reporter to approach the electrode surface, producing a large faradaic current when the electrode is interrogated using square wave voltammetry. The binding of an antibody to the epitope decreases the efficiency of this approach, producing an easily measured reduction in current. The resulting output linearly relates to the fraction of the epitope molecules bound, and thus the platform is, like ELISAs, quantitative. And because it is supported on micron-scale electrodes, it is likewise easily multiplexed[36]. Moreover, in being rapid (<15 min), single-step, and selective enough to work in blood serum, the platform also encompasses many of the promising attributes that have allowed LIAs and agglutination assays to penetrate at the point of care.

One of the first goals of this work was to improve on the raw current and signal gain of the previously published E-DNA scaffold sensor. Several modifications of the base pair complementarity and the resulting flexibility of the scaffold were investigated in the hopes of raising the raw current above the nanoamp regime and to increasing the binding-induced signal change. Based on experimental evidence, the three variations of the traditional scaffold sensor architecture explored here did not appreciably improve the raw current of the scaffold sensor. These same constructs demonstrated significantly diminished binding induced signal change in the presence of target antibody. Based on these results, it appears that original the

rigid scaffold with complete complementarity is the best choice for our E-DNA scaffold sensor architecture.

The inclusion of a secondary linear epitope to create a bivalent epitope sensor, which would increase the binding affinity and limit of detection, was similarly unsuccessful, underperforming the traditional monovalent E-DNA scaffold sensor at high and low specific antibody concentrations, for all frequency and amplitude combinations. However, this idea still has significant merit for improving the E-DNA scaffold sensor. This research only evaluated the performance of one bivalent epitope architecture, where the first linear epitope was twelve base pairs away from the electrode surface and directly underneath the second epitope. Utilization of "Y" shaped architecture where the epitopes are displayed distally, which mimics the shape of antibodies, increasing the distance of the first epitope from the electrode surface, or introducing a binding induced change in position of the redox reporter upon binding of the second epitope may yield success in creating a bivalent epitope sensor.

The second goal of this work was to expand the number of diagnostically relevant antibodies detected by the E-DNA scaffold sensor platform. To date, only the anti-gp41 E-DNA scaffold sensor has the potential to be utilized as a point of care diagnostic device. Incorporation of linear immunodominant epitopes from HCV and HSV-2 have thus far been unsuccessful. Based on experience, lack of successful integration into the E-DNA scaffold sensor stems from the following: 1) limitations in the available literature and commercial products, and 2) understanding how ELISA results inform on the success of E-DNA scaffold sensing.

Most of the literature available on the linear epitopes against diagnostically significant antibodies was done in the late 1980s and early 1990s. Initially, scientists

extensively studied and characterized linear immunodominant epitopes for diagnosis because they were cheaper and easier to produce than recombinant full-length antigens. With improvements in microfluidics, molecular imaging, protein purification and inexpensive expression vectors, serology has moved towards using full length antigens for diagnosis. Because of this, explorations of the literature to identifying linear, immunodominant epitopes usually have no follow up use/experimentation, and it is unclear if this is because other researchers did not experience the same success using the linear epitope, or if because use of this linear epitope simply became obsolete. Furthermore, identifying commercially available antibodies for use as a positive control and to determine the limit of detection is nearly impossible because characterizations of an antibody's epitope is unnecessary when using the full-length antigen for diagnosis. While one could order several different antibodies under the assumption that one of them should bind a least a portion of your linear epitope (under the assumption that, because it is immunodominant in humans, it is likely immunodominant in the organism from which the monoclonals were derived), blindly "throwing" antibodies at your linear epitope to find a good positive control is a rather expensive approach.

As we saw for the HCV scaffold sensor, and less so for HSV-2 scaffold sensor, a high signal as the result of seropositive serum in ELISA does not mean that the scaffold sensor will achieve similar results. As seen in this work, a high optical density signal in ELISA using the scaffold sensor architecture resulted in no diagnostically significant signal change electrochemically. Further work to understand this relationship, so we are better able to predict the success of incorporation of these linear epitopes into our scaffold sensors would improve experimental outcomes. Additionally, development of a high throughput method which screens multiple peptides to determine if they are immunodominant and can be

incorporated successfully into our scaffold sensing platform would be of benefit, both by reducing cost (PNAs are in the thousands of dollars) and time (PNAs take approximately 3 months to synthesize). While this was briefly explored using synthetic biotin-conjugated FLAG peptides (work not included here), these synthetic peptides were almost as expensive as PNAs and my attempts were unsuccessful.

The future of E-DNA scaffold sensors, along with the rest of diagnostic serology, is moving in the direction of using full-length or truncated antigen. Use of these biomolecules has the added benefit of presenting all (or most) of linear and conformational epitopes. Work by others in the Plaxco group have successfully demonstrated definitive diagnosis within the point of care window using scaffold sensors architectures incorporating larger antigenic fragments. To date, there has been successful detection of syphilis using truncated TPN17 and early detection of HIV-1/2 using a p24 monobody. However, until long term stability of proteins on an electrode surface can be achieved and explorations of scaffold sensor design result in diagnostically significant signal gain upon antibody binding independent of antigen size, the use of linear epitopes is still the best bet for overcoming the current limitations in point of care diagnostics with electrochemistry.

Chapter 5: Experimental

5.1 Materials

Anti-FLAG monoclonal antibody produced in mouse, anti-digoxigenin monoclonal antibody produced in mouse, 6-mercaptohexanol, sulfuric acid, bovine serum albumin, anti-human (Fc specific) IgG–peroxidase antibodies, anti-mouse (Fc specific) IgG –peroxidase antibodies 3,3',5,5'-Tetramethylbenzidine (TMB) and Tween-20 were purchased from Sigma-Aldrich (Saint Louis, MO). Clear 96 well streptavidin coated plates with bovine serum albumin blocker, human plasma fibrinogen, glycine-HCL, sodium phosphate monobasic monohydrate, sodium phosphate dibasic monohydrate, sodium hydroxide, tris (2-cholorethyl) phosphate (TCEP), UltraPure distilled water, and potassium chloride were purchased from Fisher Scientific (Saint Louis, MO). Protein G HP Spin Trap obtained from VWR International (San Francisco, CA). Amicon ultra-15 centrifugal units were obtained from Millipore Sigma (Burlington, MA). All above materials were used as received.

Human HCV positive serum samples and human serum negative for HIV, HSV-1, HSV-2, HAV, HBV, HCV, and syphilis, identified in work as "negative serum", was obtained from Biorelamation IVT (Hicksville, NY). Human HIV negative and positive serum samples for HIV types one and two were obtained from Diagnostic Biosamples (San Diego, CA). Human HSV-2 positive serum samples were obtained from Discovery Life Sciences (Los Osos, CA).

HPLC purified and lyophilized custom oligonucleotide DNA sequences with distal covalently attached variable redox reporter and terminal sulfur or biotin modifications were ordered from Biosearch Technologies (Novato, CA). HPLC purified custom oligonucleotides with a covalently attached variably positioned digoxigenin was obtained from Fidelity Oligos

(Gaithersburg, MD). All DNA stock solutions were diluted to approximately 100 μM using UltraPure distilled water and stored at -20°C in the original packaging. Peptide nucleic acid epitope chimeras were obtained from PNA Bio (Thousand Oaks, CA). All PNA stock solutions were diluted to 50.1 μM using UltraPure Distilled water and stored at -20 °C in the original packaging.

Platinum wire counter electrodes, aqueous Ag/AgCl reference electrodes, 2 mm diameter gold working electrodes were obtained from CH instruments (Bee Cave, TX). Platinum wire counter electrodes and 2mm diameter gold electrodes were used as received. Ag/AgCl reference electrodes were submerged in 3 mM KCl within the inner housing of the electrode before use.

5.2 Instrumentation

All electrochemical measurements were performed on a 1000C series multi-channel potentiostat from CH instruments (Bee Cave, TX). Enzyme linked immunosorbent assays were spectrophotometrically analyzed using a Tecan Infinite 200 PRO from Tecan (Mannedorf, Switzerland). Centrifugation was performed using a 5427 Centrifuge from Eppendorf (Hamburg, Germany). All deionized (DI) water used in methods was further purified by going through a Milli-Q Integral Water Purification System from MiliporeSigma (Burlington, MA).

5.3 DNA and PNA sequences

All DNA Sequences are written from the 5’ to the 3’ end.

DNA anchor strand used in electrochemical measurements where nucleic acids are capitalized:

(27mer): S-$(CH_2)_6$-GCA GTA ACA AGA ATA AAA CGC CAC TGC-Methylene Blue

DNA anchor stranded used in ELISA:

(27mer): Biotin-GCA GTA ACA AGA ATA AAA CGC CAC TGC

DNA complement strands used in investigation of scaffold flexibility:

Sequence 1 (Dig 1):

Digoxigenin -$(CH_2)_6$-GCA-GTG-GCG-TTT-TAT-TCT-TGT-TAC-TGC

Sequence 2 (Dig 2):

Digoxigenin-$(CH_2)_6$ -GCA-GTG-GCG-TCC-CGC-CCT-TGT-TAC-TGC

Sequence 3 (Dig 3):

Digoxigenin -$(CH_2)_6$-GCA-GTG-ATA-TTT-TAT-CTC-TGT-TAC-TGC

Sequence 4 (Dig 4):

Digoxigenin -$(CH_2)_6$-GCG-TTT-TAT-TCT

All PNA are written from the N-terminus end, where amino acids are capitalized and peptide nucleic acids are lower case:

FLAG: DYKDDDDKGG-cag tgg cgt ttt att ctt gtt act g

HIV gp41: CSGKLICTTAVPW-cag tgg cgt ttt att ctt gtt act g

HSV-2 OLD: PEEFEGAGDGEPPEDDDS-(C-S)-cagtggcgttttattcttgttactg

HSV-2 NEW: HRGGPEEFEGAGD-cag tgg cgt ttt att ctt gtt act g

HCV: MSTNPKPQKKNKRNTNRRPQDVKFPGGG – catggcgttttattcttgttactg

5.4 Methods

5.4.1 Enzyme linked immunosorbent assay

A customized ELISA was developed in our lab to utilize the same PNA-epitope chimera used in our E-DNA scaffold sensors. First, the 96 well streptavidin coated plate was washed three times with the ELISA washing buffer (1x phosphate buffered saline, 0.05% tween-20, 2% bovine serum albumin adjusted to pH 7.6 using 1 M sodium hydroxide). Next, 100 μL of biotin conjugated DNA anchor diluted in phosphate buffered saline (pH 7.6) at a concentration of 60 nM was placed into each of the wells and incubated for two hours . The plate was then washed three times with washing buffer before each well was incubated with 100 μL of 200 nM PNA diluted in phosphate buffered saline (pH 7.6) for one hour. The plate was then washed three times with the washing buffer before 100 μL of variable dilutions (1:1000 to 1:10 dilution) of human serum in washing buffer were placed in the wells (per experimental design) and allowed to incubate for one hour. Following an additional six washes with washing buffer, 100 μL of 1:15000 diluted peroxidase conjugated secondary antibody (either anti-human or anti-mouse, per experimental design) in washing buffer was placed into each of the wells for an incubation of thirty minutes. The plate was again washed five times before each well was incubated with 100 μL of TMB substrate. Color from the peroxidase-TMB reaction was allowed to develop before the reaction was stopped with 50 μL of 2 M sulfuric acid. Results were evaluated by averaging the absorption of each well at 450 nm for 25 flashes of light using the Tecan Microplate reader.

All experiments were repeated triplicate using separate wells. ELISA data presented figures is the average of those three wells and with error bars representing one standard deviation.

5.4.2 Electrochemical Measurements

Prior to building the E-DNA scaffold on the surface, the 2 mm diameter gold electrodes were mechanically polished using a 0.05 μm aluminum oxide slurry. The electrodes were then electrochemically cleaned in the following steps: 1) a reductive desorption of any organic contaminants using cyclic voltammetry in 0.5 M sodium hydroxide, 3) potential cycling in 0.5 M sulfuric acid using cyclic voltammetry to further remove organic contaminants while forming and reducing a gold oxide layer, 3) chloride etching to further clean the gold surface using 0.1 M sulfuric acid and 0.01 M potassium chloride, and 4) complete reduction of the gold surface in 0.05 M sulfuric acid using cyclic voltammetry. The electrodes are then rinsed with DI water before building the scaffold sensor on the clean, reduced gold surface.

Following mechanical and electrochemical cleaning, the electrodes are placed in 100 μL of variable concentrations of the DNA anchor solution (per experimental design) with a terminal thiol that has been reduced over the course of an hour to prevent any disulfide bonds TCEP (10 mM in DI water). After incubating with the DNA anchor for one hour at room temperature (~25 °C), electrode was placed into 100 μL of 5 mM 6-mercaptohexanol in DI water where it was incubated overnight (12-16 hours) at 4 °C. The next day electrodes were placed in 100 μL of the requisite PNA with a concentration of at least four times the concentration of anchor strand and incubated for two hours.

Working electrodes with the scaffold sensor and SAM on the surface, the platinum counter electrode, and the Ag/AgCl reference electrode were then connected to the potentiostat. These electrodes were submerged in a blocking solution (3x phosphate buffered saline, 0.05% tween-20, and 1% fibrinogen) and allowed to equilibrate for 20 minutes. Following this equilibration step, electrodes were then challenged with variable dilutions (1:1000 to 1:10 dilution) of patient serum or monoclonal antibody by direct addition into the blocking solution, depending on experimental design. Alternatively, electrodes were blocked with the above-mentioned blocking solution, before additional blocking using variable dilutions (1:40 to 1:10) of known negative human serum before being challenged with dilute positive serum or monoclonal antibody. All experiments were performed square wave voltammetry (approximately one scan/minute) with a frequency of 60 Hz and an amplitude of 0.25 mV between -0.05 and -0.45, which is the potential window for the reduction of methylene blue relative to the Ag/AgCl reference.

Frequency-amplitude tuning was performed using continuous scanning (variable time between scans on each based on frequency) by square wave voltammetry in 3x phosphate buffered saline (pH 7.6) at a range of 1-500 Hz and 10-100 mV, respectively. After cycling through designated frequency amplitude pairs within the above ranges, the electrodes were again scanned under the same square wave voltammetry conditions after 30 minutes of equilibration with target serum (1:10 dilution) or monoclonal antibody at saturating concentrations.

All experiments were repeated triplicate using separate electrodes. Electrochemical data presented figures is the average of those three electrodes and with error bars representing one standard deviation.

5.4.3 Data Analysis

Electrochemical data:

Data collected from the electrochemical experiments conducted on the CH instruments multichannel potentiostat were analyzed using MatLab (Natick, MA). In brief, data from electrochemical experiments was converted into a test file that was accessed by MatLab. At MatLab script was then applied to the data file, which created a flat baseline by connecting points on either side of the reduction peak as designated by the user (typically between approximately -0.15 and -0.35 V). The program then determined the maximum current within the given interval and subtracted the baseline current, which yields the current for that electrode. This data was then imported into Microsoft Excel (Redmond, WA), where change in current as a function of time after exposure to either blocking conditions or positive or negative serum was determined. The percent change in was current was determined by performed by subtracting the starting current (before challenge) with the current challenge, diving by the starting current, and then multiplying by 100. Electrode changes in signal for triplicate measurements were then averaged and the standard deviation was determined.

ELISA Data:

Data collected via the Tecan multiplate reader was analyzed using Microsoft Excel. The triplicate experimental conditions were averaged, and the standard deviation was calculated.

Chapter 6: References

1. Gaydos, C. & Hardick, J. Point of care diagnostics for sexually transmitted infections: perspectives and advances. *Expert Rev. Anti Infect. Ther.* 12, 657–672 (2014).
2. Peeling, R. W., Holmes, K. K., Mabey, D. & Ronald, A. Rapid tests for sexually transmitted infections (STIs): the way forward. *Sex. Transm. Infect.* 82, v1–v6 (2006).
3. Anfossi, L., Di Nardo, F., Cavalera, S., Giovannoli, C. & Baggiani, C. Multiplex Lateral Flow Immunoassay: An Overview of Strategies towards High-throughput Point-of-Need Testing. *Biosensors* 9, 2 (2018).
4. Grant, M. S. The effect of blood drawing techniques and equipment on the hemolysis of ED laboratory blood samples. *J. Emerg. Nurs.* 29, 116–121 (2003).
5. Performance of Anyplex™ II multiplex real-time PCR for the diagnosis of seven sexually transmitted infections: comparison with currently available methods | Elsevier Enhanced Reader. doi:10.1016/j.ijid.2013.07.011
6. *Herpes simplex virus type 2: programmatic and research priorities in developing countries : report of a WHO/UNAIDS/LSHTM workshop (London, 14-16 February 2001).* (World Health Organization : Joint United Nations Programme on HIV/AIDS, 2001).
7. Sillanpaa, M. *et al.* Hepatitis C virus core, NS3, NS4B and NS5A are the major immunogenic proteins in humoral immunity in chronic HCV infection. *Virol. J.* 6, 84 (2009).
8. Edited on behalf of the National Institute of Biomedical Imaging and Bioengineering/National Heart, Lung, and Blood Institute/National Science Foundation

Workshop Faculty, Price, C. P. & Kricka, L. J. Improving Healthcare Accessibility through Point of care Technologies. *Clin. Chem.* 53, 1665–1675 (2007).

9. Junker, R., Schlebusch, H. & Luppa, P. B. Point of care Testing in Hospitals and Primary Care. *Dtsch. Aerzteblatt Online* (2010). doi:10.3238/arztebl.2010.0561
10. Dugdale, D. C., Epstein, R. & Pantilat, S. Z. Time and the patient-physician relationship. *J. Gen. Intern. Med.* 14, S34–S40 (1999).
11. Baum, L. L. Role of Humoral Immunity in Host Defense Against HIV. *Curr. HIV/AIDS Rep.* 7, 11–18 (2010).
12. Wang, W., Singh, S., Zeng, D. L., King, K. & Nema, S. Antibody Structure, Instability, and Formulation. *J. Pharm. Sci.* 96, 1–26 (2007).
13. Bahadır, E. B. & Sezgintürk, M. K. Lateral flow assays: Principles, designs and labels. *TrAC Trends Anal. Chem.* 82, 286–306 (2016).
14. Ortega-Vinuesa, J. L. & Bastos-González, D. A review of factors affecting the performances of latex agglutination tests. *J. Biomater. Sci. Polym. Ed.* 12, 379–408 (2001).
15. Gordon, J. & Michel, G. Analytical Sensitivity Limits for Lateral Flow Immunoassays. *Clin. Chem.* 54, 1250–1251 (2008).
16. Parolo, C., de la Escosura-Muñiz, A. & Merkoçi, A. Enhanced lateral flow immunoassay using gold nanoparticles loaded with enzymes. *Biosens. Bioelectron.* 40, 412–416 (2013).
17. White, R. J. *et al.* Wash-free, Electrochemical Platform for the Quantitative, Multiplexed Detection of Specific Antibodies. *Anal. Chem.* 84, 1098–1103 (2012).

18. Zaiko, V. V. *et al.* Microarray method for multiplex and serial latex agglutination tests with digital image registration. *Clin. Lab.* 54, 273–279 (2008).
19. World Health Organization, World Health Organization & Global Hepatitis Programme. *Global hepatitis report, 2017*. (2017).
20. Kim, M. H., Kang, S. Y. & Lee, W. I. Evaluation of a new rapid test kit to detect hepatitis C virus infection. *J. Virol. Methods* 193, 379–382 (2013).
21. Andreotti, P. E. *et al.* Immunoassay of infectious agents. *BioTechniques* 35, 850–859 (2003).
22. Smith, D. S. & Eremin, S. A. Fluorescence polarization immunoassays and related methods for simple, high-throughput screening of small molecules. *Anal. Bioanal. Chem.* 391, 1499–1507 (2008).
23. Chan, C. P. Y. *et al.* Evidence-Based Point of care Diagnostics: Current Status and Emerging Technologies. *Annu. Rev. Anal. Chem.* 6, 191–211 (2013).
24. Frisk, T. *et al.* An integrated QCM-based narcotics sensing microsystem. *Lab. Chip* 8, 1648–1657 (2008).
25. Vaisocherová, H. *et al.* Surface plasmon resonance biosensor for direct detection of antibody against Epstein-Barr virus. *Biosens. Bioelectron.* 22, 1020–1026 (2007).
26. Sakata, T., Matsumoto, S., Nakajima, Y. & Miyahara, Y. Potential Behavior of Biochemically Modified Gold Electrode for Extended-Gate Field-Effect Transistor. *Jpn. J. Appl. Phys.* 44, 2860–2863 (2005).
27. Lequin, R. M. Enzyme Immunoassay (EIA)/Enzyme-Linked Immunosorbent Assay (ELISA). *Clin. Chem.* 51, 2415–2418 (2005).

28. Dixit, C. K. *et al.* Development of a High Sensitivity Rapid Sandwich ELISA Procedure and Its Comparison with the Conventional Approach. *Anal. Chem.* 82, 7049–7052 (2010).

29. Ashley, R. L. Sorting out the new HSV type specific antibody tests. *Sex. Transm. Infect.* 77, 232–237 (2001).

30. Saville, R. D. *et al.* Fourth-Generation Enzyme-Linked Immunosorbent Assay for the Simultaneous Detection of Human Immunodeficiency Virus Antigen and Antibody. *J. Clin. Microbiol.* 39, 2518–2524 (2001).

31. Rowe, A. A., White, R. J., Bonham, A. J. & Plaxco, K. W. Fabrication of Electrochemical-DNA Biosensors for the Reagentless Detection of Nucleic Acids, Proteins and Small Molecules. *J. Vis. Exp.* 2922 (2011). doi:10.3791/2922

32. Pensa, E. *et al.* The Chemistry of the Sulfur–Gold Interface: In Search of a Unified Model. *Acc. Chem. Res.* 45, 1183–1192 (2012).

33. Kang, D., Ricci, F., White, R. J. & Plaxco, K. W. Survey of Redox-Active Moieties for Application in Multiplexed Electrochemical Biosensors. *Anal. Chem.* 88, 10452–10458 (2016).

34. Li, H. *et al.* A Biomimetic Phosphatidylcholine-Terminated Monolayer Greatly Improves the In Vivo Performance of Electrochemical Aptamer-Based Sensors. *Angew. Chem. Int. Ed.* 56, 7492–7495 (2017).

35. Xiao, Y., Uzawa, T., White, R. J., DeMartini, D. & Plaxco, K. W. On the Signaling of Electrochemical Aptamer-Based Sensors: Collision- and Folding-Based Mechanisms. *Electroanalysis* 21, 1267–1271 (2009).

36. Cash, K. J., Ricci, F. & Plaxco, K. W. An Electrochemical Sensor for the Detection of Protein−Small Molecule Interactions Directly in Serum and Other Complex Matrices. *J. Am. Chem. Soc.* 131, 6955–6957 (2009).
37. Kang, D. *et al.* Expanding the Scope of Protein-Detecting Electrochemical DNA "Scaffold" Sensors. *ACS Sens.* 3, 1271–1275 (2018).
38. Kawaguchi, T. *et al.* Fabrication of a novel immunosensor using functionalized self-assembled monolayer for trace level detection of TNT by surface plasmon resonance. *Talanta* 72, 554–560 (2007).
39. Ziegler, C. Cantilever-based biosensors. *Anal. Bioanal. Chem.* 379, (2004).
40. Patterson, A. S. Rapid, single-step measurement of specific antibodies in patient serum using the electrochemical DNA sensor. *Unpublished* Available at: https://docs.google.com/document/d/1G0LqE6rBsR8l6_6lyhloJ7cTpnPmK2NtAjXHUFO6Pnk/edit?usp=drive_web&ouid=110227334514471556886&usp=embed_facebook. (Accessed: 30th May 2019)
41. Ebina, W., Rowat, A. C. & Weitz, D. A. Electrodes on a budget: Micropatterned electrode fabrication by wet chemical deposition. *Biomicrofluidics* 3, 034104 (2009).
42. Rowe, A. A. *et al.* CheapStat: An Open-Source, "Do-It-Yourself" Potentiostat for Analytical and Educational Applications. *PLoS ONE* 6, e23783 (2011).
43. World Health Organization. *World health statistics 2018: monitoring health for the SDGs*. (2018).
44. Farr, S. L., Kraft, J. M., Warner, L., Anderson, J. E. & Jamieson, D. J. The integration of STD/HIV services with contraceptive services for young women in the United States. *Am. J. Obstet. Gynecol.* 201, 142.e1-142.e8 (2009).

45. Nationally representative CDC study finds 1 in 4 teenage girls has a sexually transmitted disease. (2008). doi:10.1037/e455382008-001
46. Einhauer, A. & Jungbauer, A. The FLAGe peptide, a versatile fusion tag for the purification of recombinant proteins. 11 (2001).
47. Uzawa, T., Cheng, R. R., White, R. J., Makarov, D. E. & Plaxco, K. W. A Mechanistic Study of Electron Transfer from the Distal Termini of Electrode-Bound, Single-Stranded DNAs. *J. Am. Chem. Soc.* 132, 16120–16126 (2010).
48. Dauphin-Ducharme, P. & Plaxco, K. W. Maximizing the Signal Gain of Electrochemical-DNA Sensors. *Anal. Chem.* 88, 11654–11662 (2016).
49. Rowe, A. A. *et al.* Electrochemical Biosensors Employing an Internal Electrode Attachment Site and Achieving Reversible, High Gain Detection of Specific Nucleic Acid Sequences. *Anal. Chem.* 83, 9462–9466 (2011).
50. Sosnick, T. R., Benjamin, D. C., Novotny, J., Seeger, P. A. & Trewhella, J. Distances between the antigen-binding sites of three murine antibody subclasses measured using neutron and x-ray scattering. *Biochemistry* 31, 1779–1786 (1992).
51. Huppert, J., Hesse, E. & Gaydos, C. A. What Is the Point? How Point of care Sexually Transmitted Infection Tests Can Impact Infected Patients: *Point Care J. -Patient Test. Technol.* 9, 36–46 (2010).
52. *Herpes simplex virus type 2: programmatic and research priorities in developing countries : report of a WHO/UNAIDS/LSHTM workshop (London, 14-16 February 2001).* (World Health Organization : Joint United Nations Programme on HIV/AIDS, 2001).

53. Walensky, R. P. *et al.* Scaling Up the 2010 World Health Organization HIV Treatment Guidelines in Resource-Limited Settings: A Model-Based Analysis. *PLoS Med.* 7, e1000382 (2010).

54. Arakawa, T., Prestrelski, S. J., Kenney, W. C. & Carpenter, J. F. Factors affecting short-term and long-term stabilities of proteins. *Adv. Drug Deliv. Rev.* 20 (2001).

55. WHO | Progress report on HIV, viral hepatitis and sexually transmitted infections 2019. *WHO* Available at: http://www.who.int/hiv/strategy2016-2021/progress-report-2019/en/. (Accessed: 27th May 2019)

56. Busch, M. P. & Satten, G. A. Time course of viremia and antibody seroconversion following human immunodeficiency virus exposure. *Am. J. Med.* 102, 117–124 (1997).

57. Fact Sheet 1 HIV. Available at: https://www.who.int/hiv/abouthiv/fact_sheet_hiv.htm. (Accessed: 27th May 2019)

58. Daar, E. S. *et al.* Diagnosis of Primary HIV-1 Infection. 5

59. Palacios-Rodríguez, Y., Gazarian, T., Rowley, M., Majluf-Cruz, A. & Gazarian, K. Collection of phage–peptide probes for HIV-1 immunodominant loop-epitope. *J. Microbiol. Methods* 68, 225–235 (2007).

60. WHO | Point of care Diagnostic Tests (POCTs) for Sexually Transmitted Infections (STIs). *WHO* Available at: http://www.who.int/reproductivehealth/topics/rtis/pocts/en/. (Accessed: 27th May 2019)

61. Shepard, C. W., Finelli, L. & Alter, M. J. Global epidemiology of hepatitis C virus infection. *Lancet Infect. Dis.* 5, 558–567 (2005).

62. Gupta, E., Bajpai, M. & Choudhary, A. Hepatitis C virus: Screening, diagnosis, and interpretation of laboratory assays. *Asian J. Transfus. Sci.* 8, 19 (2014).

63. Alter, M. J., Kuhnert, W. L., Finelli, L. & Centers for Disease Control and Prevention. Guidelines for laboratory testing and result reporting of antibody to hepatitis C virus. Centers for Disease Control and Prevention. *MMWR Recomm. Rep. Morb. Mortal. Wkly. Rep. Recomm. Rep.* 52, 1–13, 15; quiz CE1-4 (2003).
64. WHO | First WHO prequalified hepatitis C rapid test opens the door to expanded treatment. *WHO* Available at: http://www.who.int/medicines/news/prequal_hvc/en/. (Accessed: 27th May 2019)
65. Sallberg, Ma. Immunodominant Regions within the Hepatitis C Virus Core and Putative Matrix Proteins. *J CLIN MICROBIOL* 30, 6 (1992).
66. Buratti, E. *et al.* Improved Reactivity of Hepatitis C Virus Core Protein Epitopes in a Conformational Antigen-Presenting System. *CLIN DIAGN LAB IMMUNOL* 4, 5 (1997).
67. Sallberg, Ma. Immunodominant Regions within the Hepatitis C Virus Core and Putative Matrix Proteins. *J CLIN MICROBIOL* 30, 6 (1992).
68. Goeser, T., Müller, H. M., Ye, J., Pfaff, E. & Theilmann, L. Characterization of Antigenic Determinants in the Core Antigen of the Hepatitis C Virus. *Virology* 205, 462–469 (1994).
69. Ross, J. D., Smith, I. W. & Elton, R. A. The epidemiology of herpes simplex types 1 and 2 infection of the genital tract in Edinburgh 1978-1991. *Genitourin. Med.* 69, 381–383 (1993).
70. Langenberg, A. Development of Clinically Recognizable Genital Lesions among Women Previously Identified as Having ‘Asymptomatic’ Herpes Simplex Virus Type 2 Infection. *Ann. Intern. Med.* 110, 882 (1989).

71. Langenberg, A. G. M., Corey, L., Ashley, R. L., Leong, W. P. & Straus, S. E. A Prospective Study of New Infections with Herpes Simplex Virus Type 1 and Type 2. *N. Engl. J. Med.* 341, 1432–1438 (1999).

72. Levi, M. Peptide Sequences of Glycoprotein G-2 Discriminate between Herpes Simplex Virus Type 2 (HSV-2) and HSV-1 Antibodies. *CLIN DIAGN LAB IMMUNOL* 3, 5 (1996).

73. Sj√∂gren-Jansson, E. *et al.* Localization of type-specific epitopes of herpes simplex virus type 2 glycoprotein G recognized by human and mouse antibodies. *J. Gen. Virol.* 79, 1215–1224 (1998).

74. Laderman, E. I. *et al.* Rapid, Sensitive, and Specific Lateral-Flow Immunochromatographic Point of care Device for Detection of Herpes Simplex Virus Type 2-Specific Immunoglobulin G Antibodies in Serum and Whole Blood. *Clin. Vaccine Immunol.* 15, 159–163 (2008).

75. Binger, A. M. E.-H., Umer, M. D., Matz, B. & Schneweis, K. E. Evaluation of Three Glycoprotein G2-Based Enzyme Immunoassays for Detection of Antibodies to Herpes Simplex Virus Type 2 in Human Sera. 37, 5 (1999).

76. Marsden, H. S., MacAulay, K., Murray, J. & Smith, I. W. Identification of an immunodominant sequential epitope in glycoprotein G of herpes simplex virus type 2 that is useful for serotype-specific diagnosis. *J. Med. Virol.* 56, 79–84 (1998).

77. Nilsen, A. *et al.* Performance characteristics of a glycoprotein G based oligopeptide (peptide 55) and two different methods using the complete glycoprotein as assays for detection of anti-HSV-2 antibodies in human sera. *J. Virol. Methods* 107, 21–27 (2003).

78. Oladepo, D. K., Klapper, P. E. & Marsden, H. S. Peptide based enzyme-linked immunoassays for detection of anti-HSV-2 IgG in human sera. *J. Virol. Methods* 87, 63–70 (2000).

79. Liljeqvist, J. *et al.* Localization of type-specific epitopes of herpes simplex virus type 2 glycoprotein G recognized by human and mouse antibodies. *J. Gen. Virol.* 79 (Pt 5), 1215–24 (1998).

80. Paull, M. L. & Daugherty, P. S. Mapping serum antibody repertoires using peptide libraries. *Curr. Opin. Chem. Eng.* 19, 21–26 (2018).

81. Wang, J. Electrochemical biosensors: Towards point of care cancer diagnostics. *Biosens. Bioelectron.* 21, 1887–1892 (2006).